

Supplementary information

Construction of giant glycosidase inhibitors from iminosugar-substituted fullerene macromonomers

Thi Minh Nguyet Trinh,^a Michel Holler,^a Jérémy P. Schneider,^b M. Isabel García-Moreno,^c
José M. García Fernández,^d Anne Bodlenner,^b Philippe Compain,^{*b} Carmen Ortiz Mellet,^{*c}
and Jean-François Nierengarten^{*a}

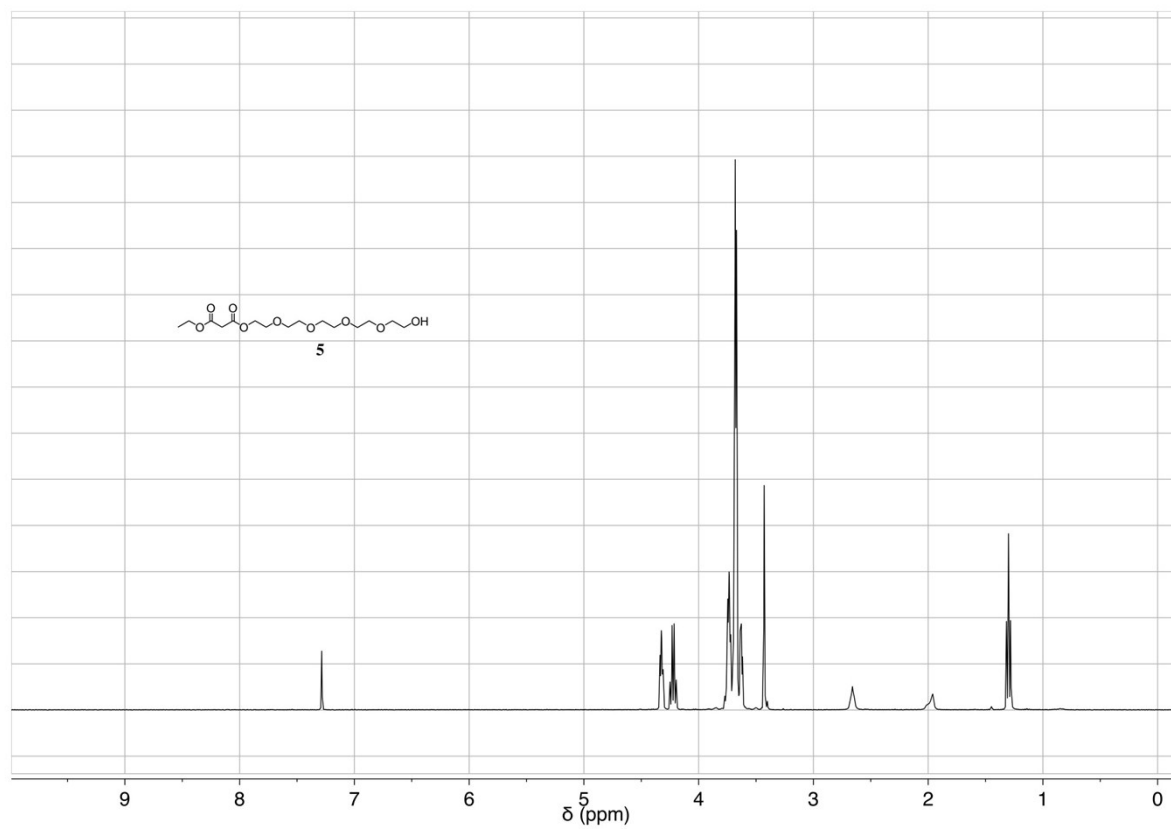


Figure S1a. ¹H NMR spectrum of compound 5 (CDCl₃, 400 MHz).

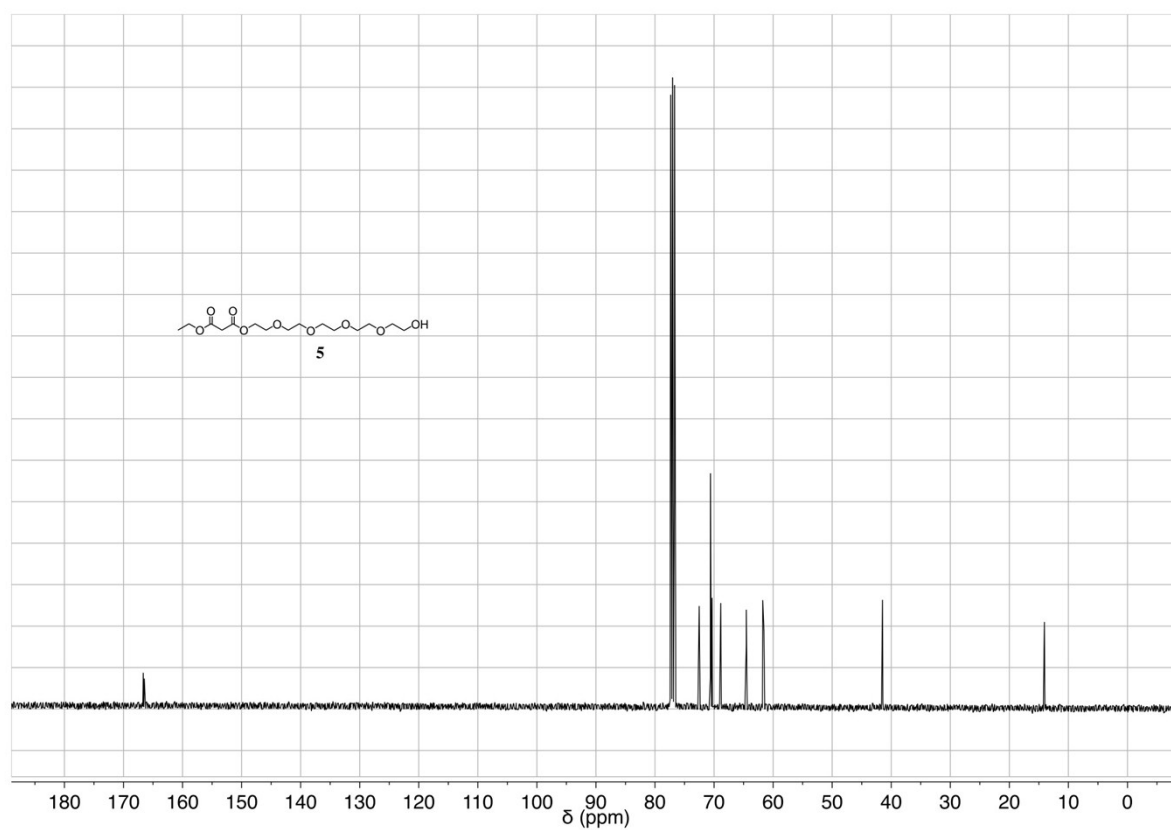


Figure S1b. ^{13}C NMR spectrum of compound **5** (CDCl_3 , 100 MHz).

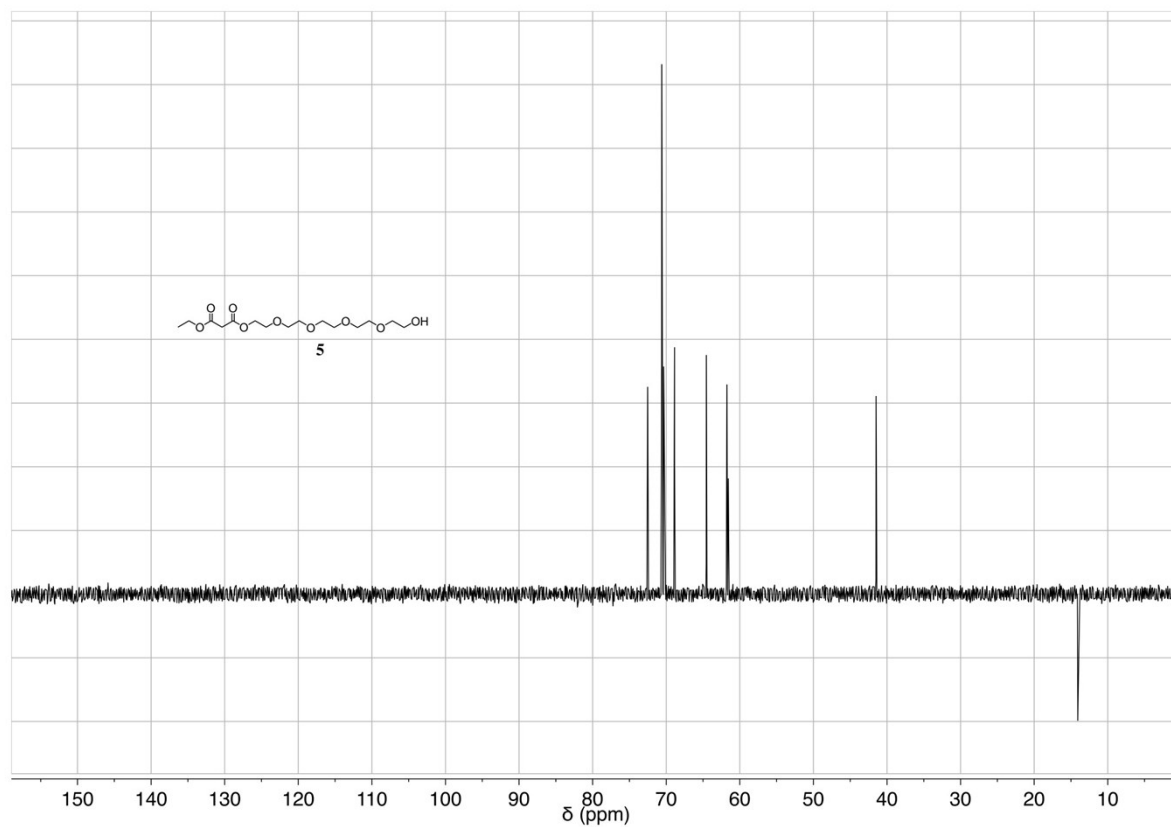


Figure S1c. DEPT spectrum of compound **5** (CDCl_3 , 100 MHz).

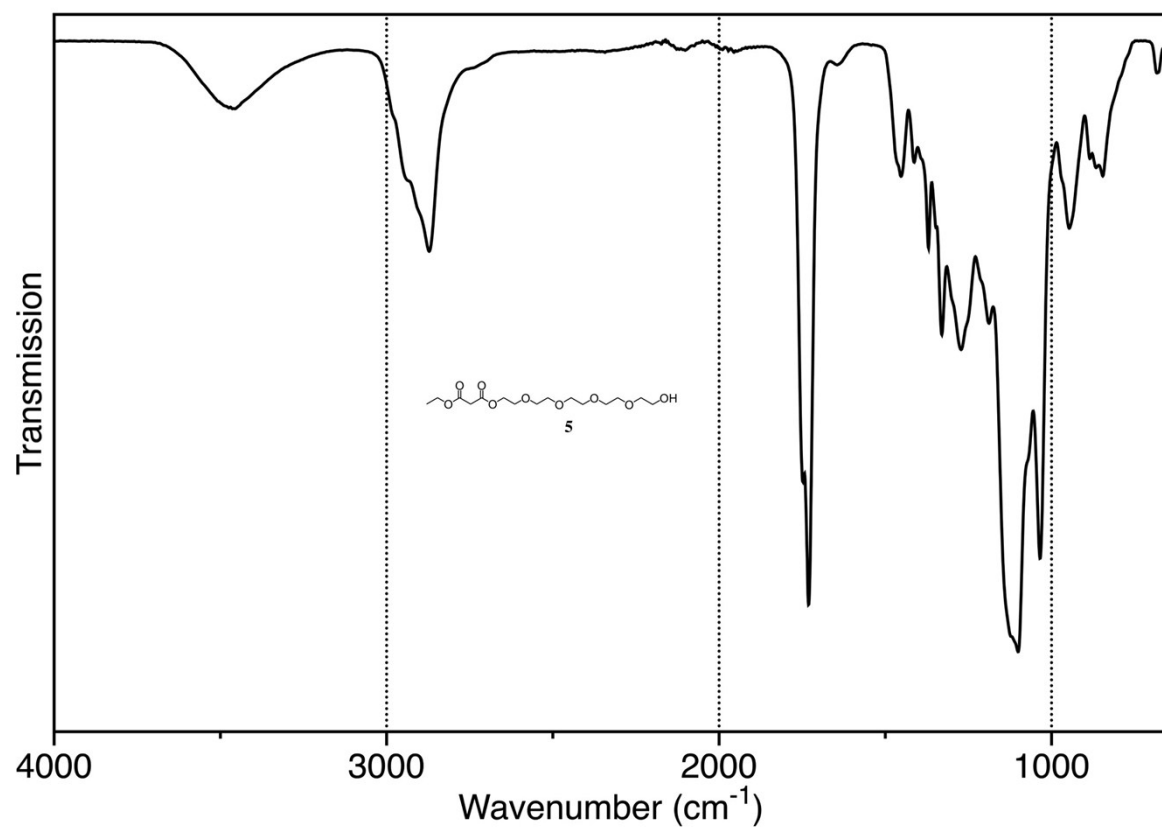


Figure S1d. IR spectrum of compound 5.

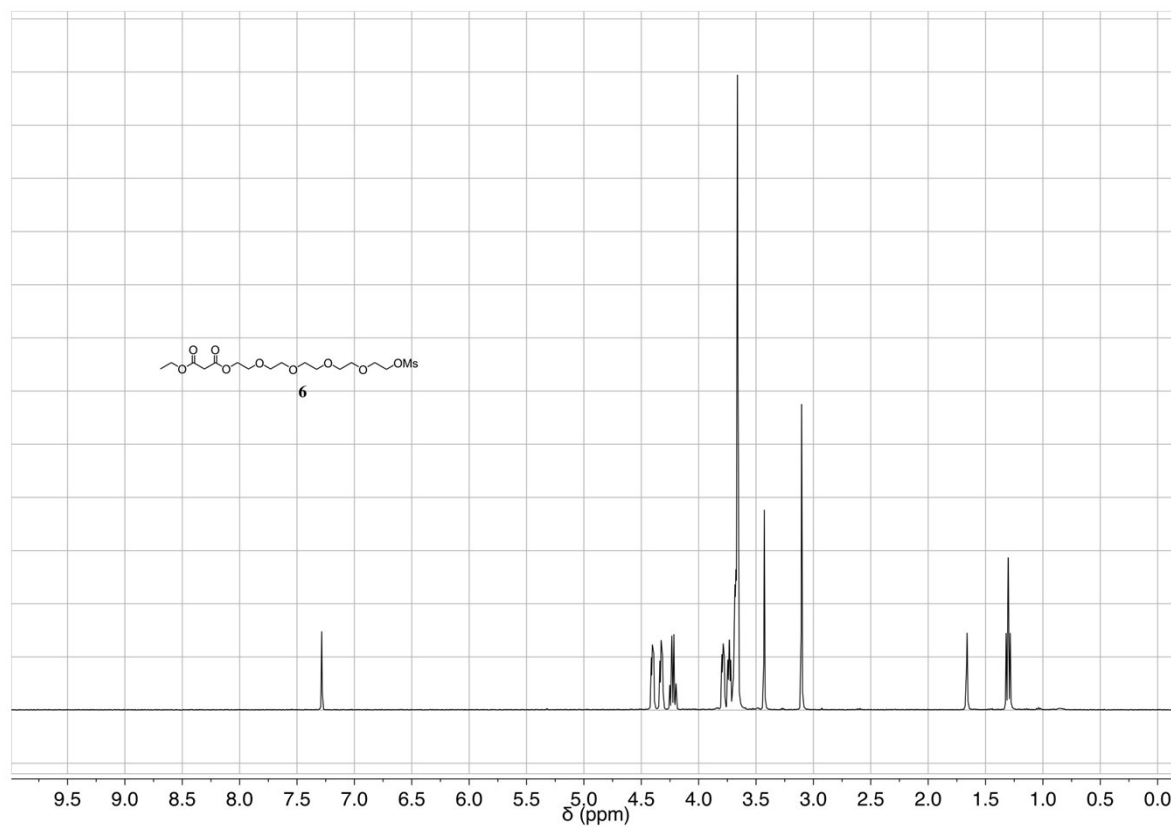


Figure S2a. ¹H NMR spectrum of compound **6** (CDCl₃, 400 MHz).

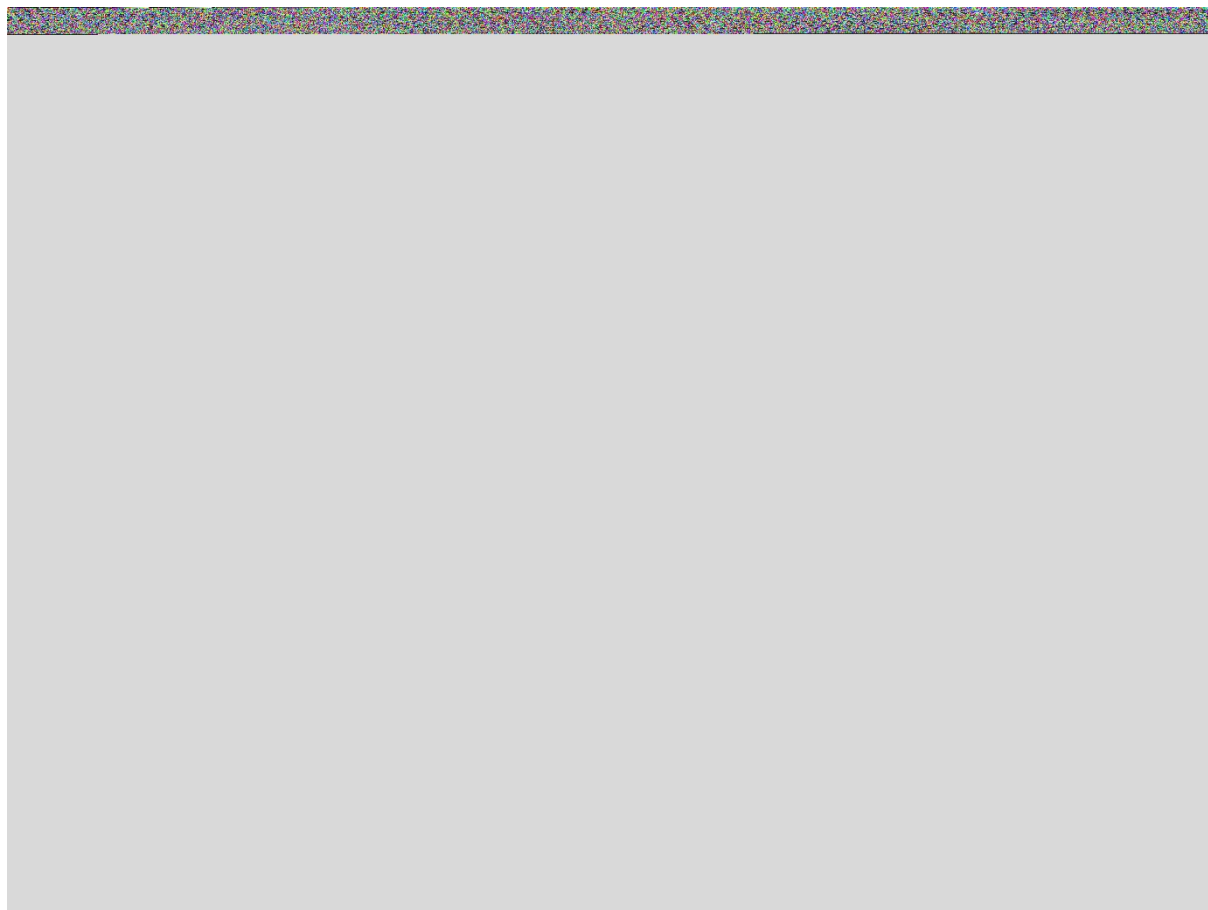


Figure S2b. ¹³C NMR spectrum of compound **6** (CDCl₃, 100 MHz).

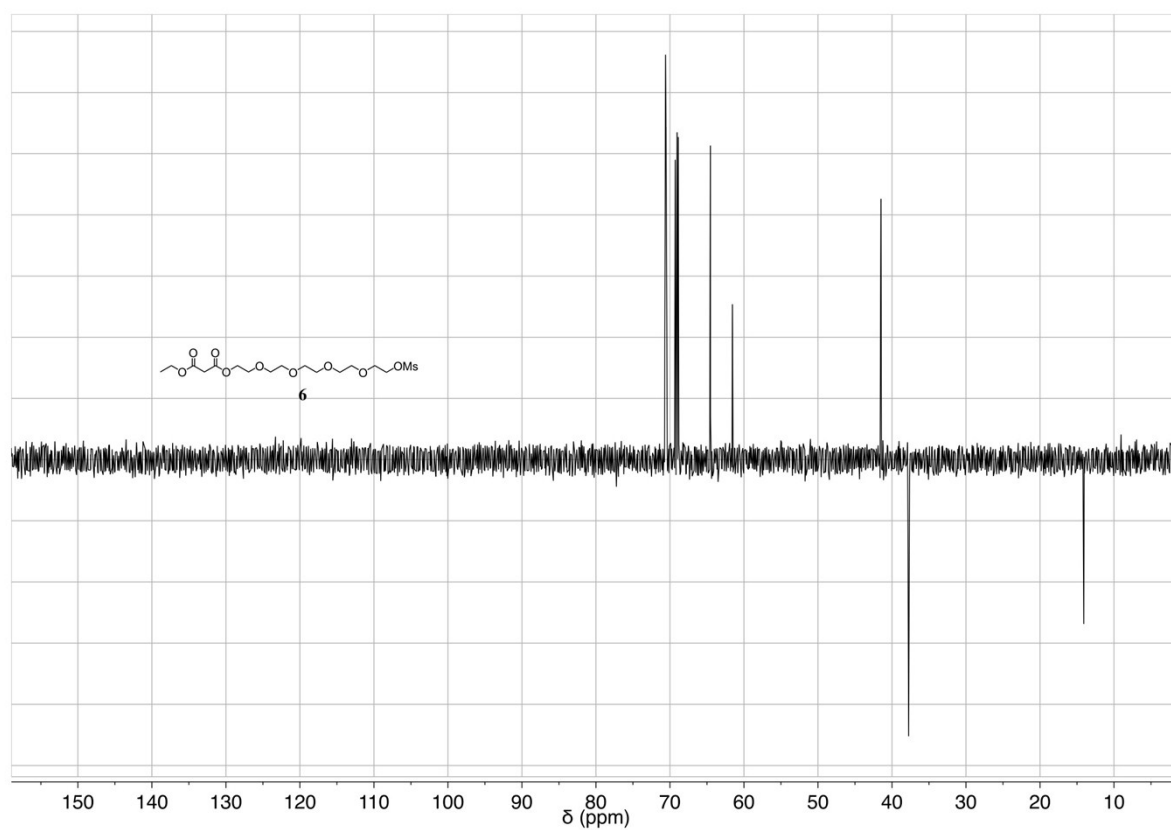


Figure S2c. DEPT spectrum of compound **6** (CDCl_3 , 100 MHz).

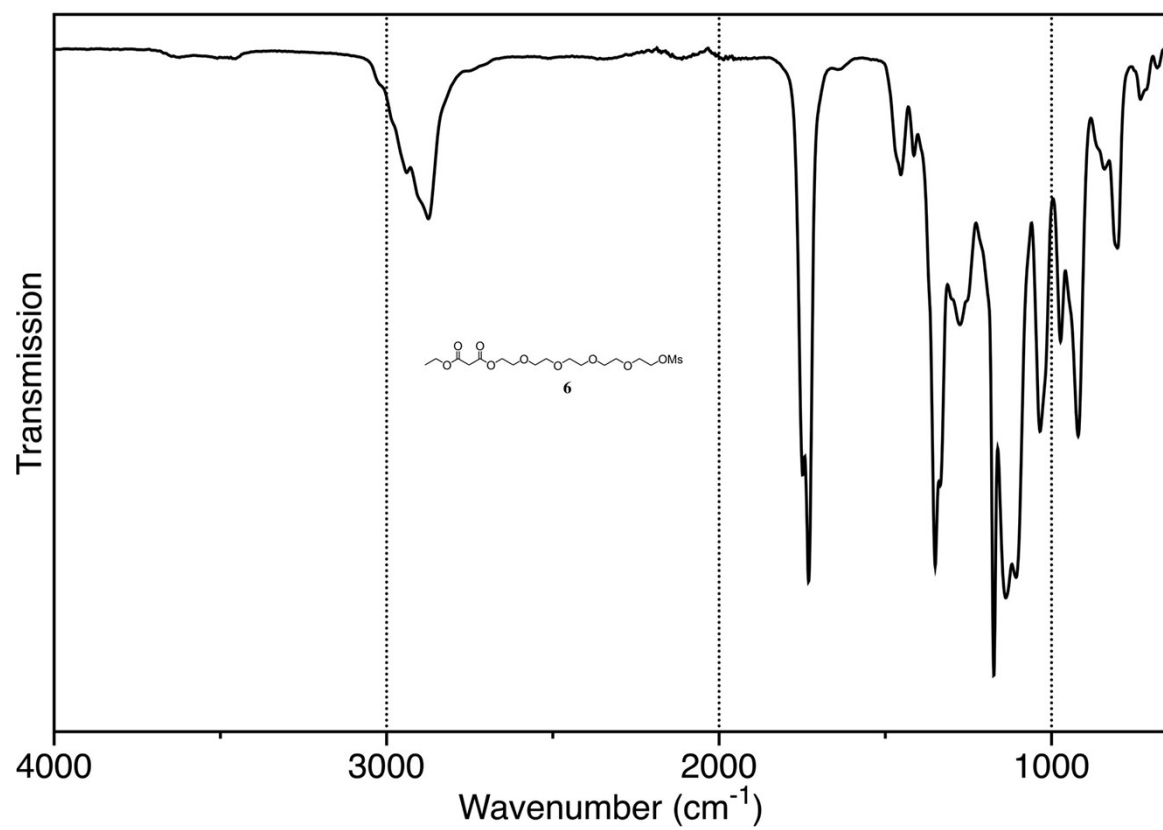


Figure S2d. IR spectrum of compound 6.

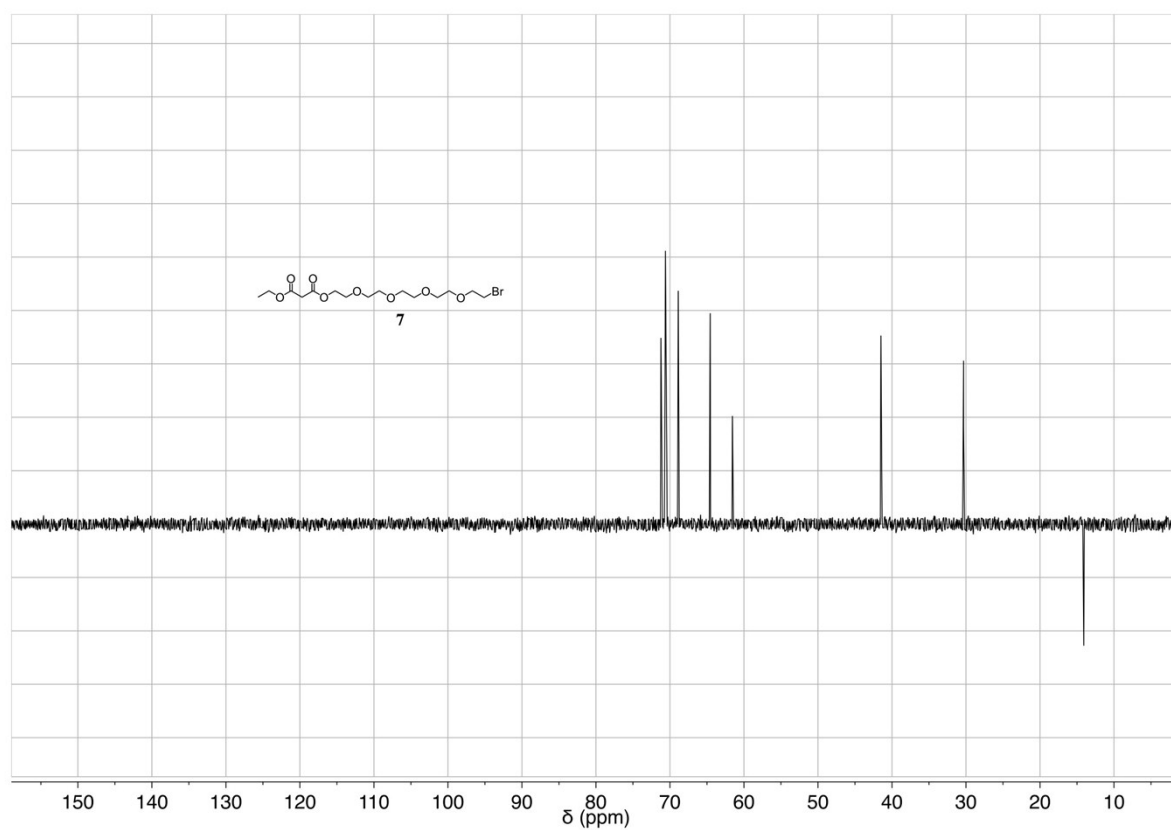


Figure S3c. DEPT spectrum of compound 7 (CDCl_3 , 100 MHz).

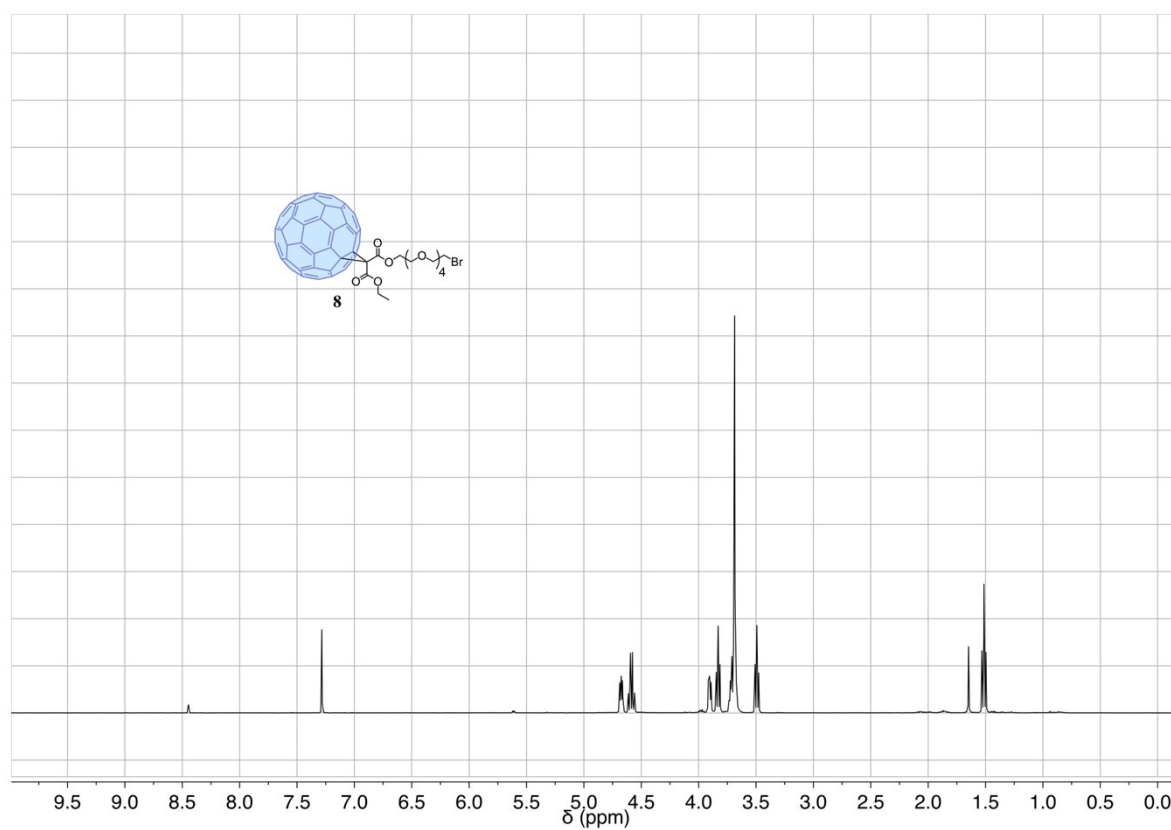


Figure S4a. ¹H NMR spectrum of compound **8** (CDCl₃, 400 MHz).

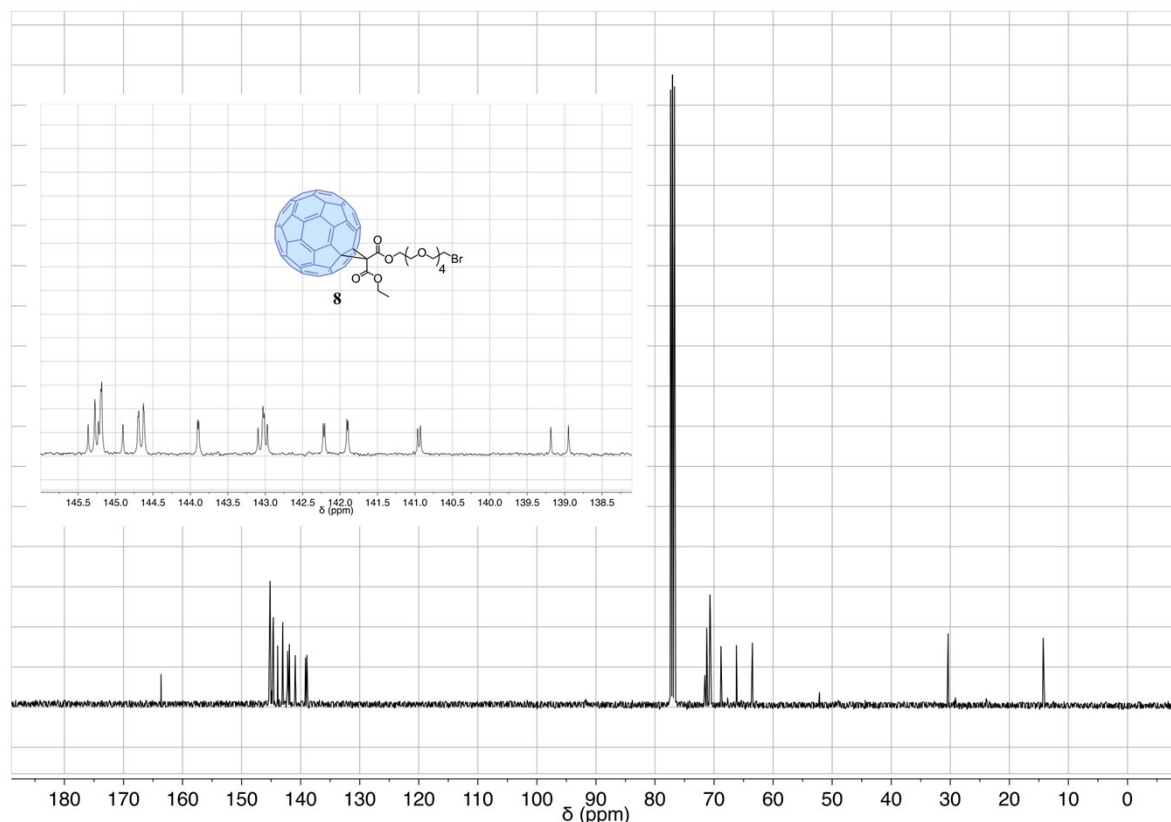


Figure S4b. ^{13}C NMR spectrum of compound **8** (CDCl_3 , 100 MHz). Close inspection of the fullerene signals revealed a strong influence of the local symmetry. In the ^{13}C NMR spectrum of mono-adduct **8**, only 24 fullerene signals are observed out of the 32 expected ones for a C_5 -symmetrical derivative (31 for the fullerene sp^2 carbon atoms and one for the two equivalent fullerene sp^3 C atoms). Actually compound **8** possess a pseudo- C_{2v} symmetry and the pattern for the fullerene signals observed for **8** is reminiscent to the one typically seen for a C_{2v} -symmetrical methanofullerene derivative with two equivalent ester moieties.

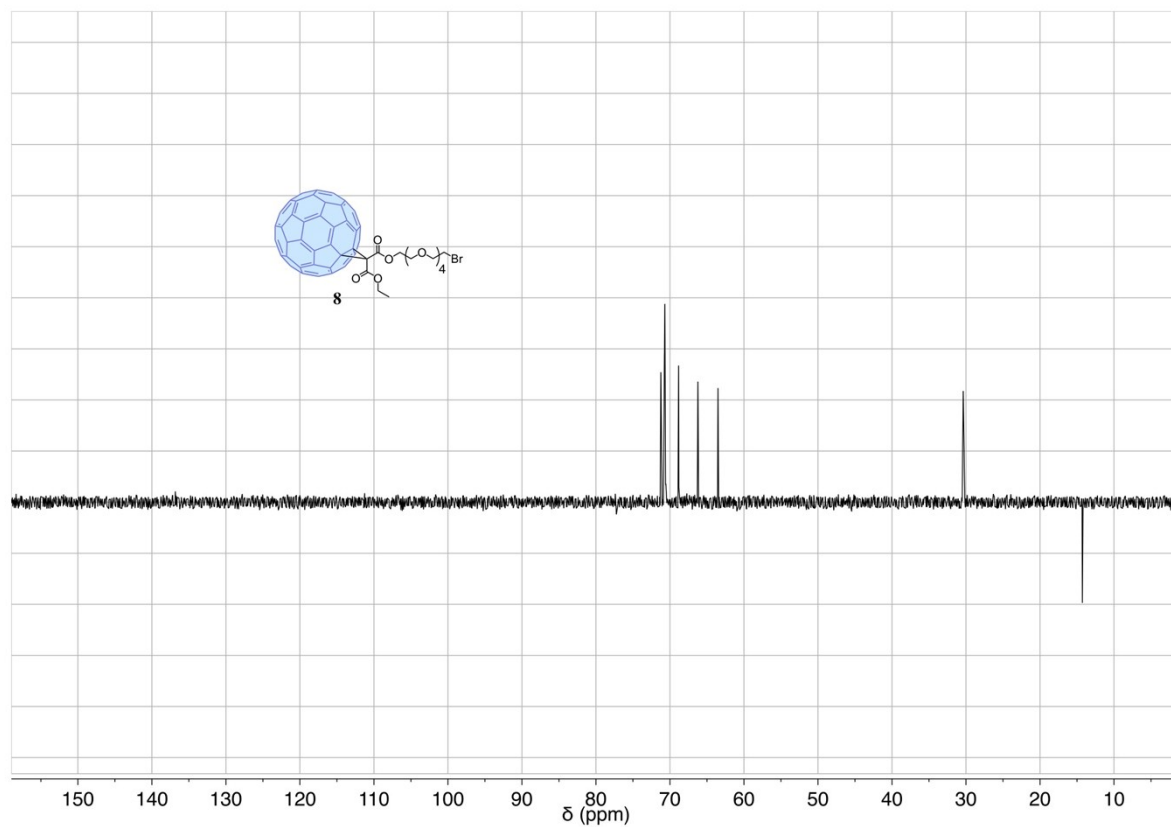


Figure S4c. DEPT spectrum of compound **8** (CDCl₃, 100 MHz).

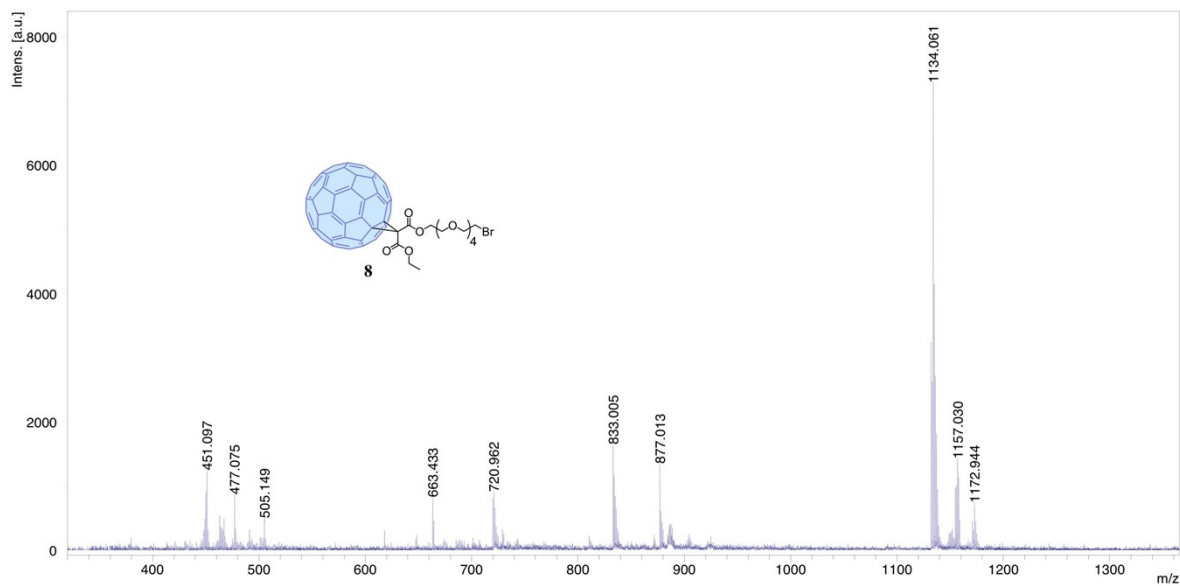


Figure S4d. MALDI TOF mass spectrum of compound **8**: 1172.9 ($[M+K]^+$), 1157.0 ($[M+Na]^+$), 1134.0 ($[M]^+$), 877.0 ($[M-HOCH_2(CH_2OCH_2)_3CH_2Br]^+$), 833.0 ($[M-OCH_2(CH_2OCH_2)_4CH_2Br]^+$), 720.9 ($[C_{60}]^+$), 451.1 ($[M-C_{60}+K]^+$).

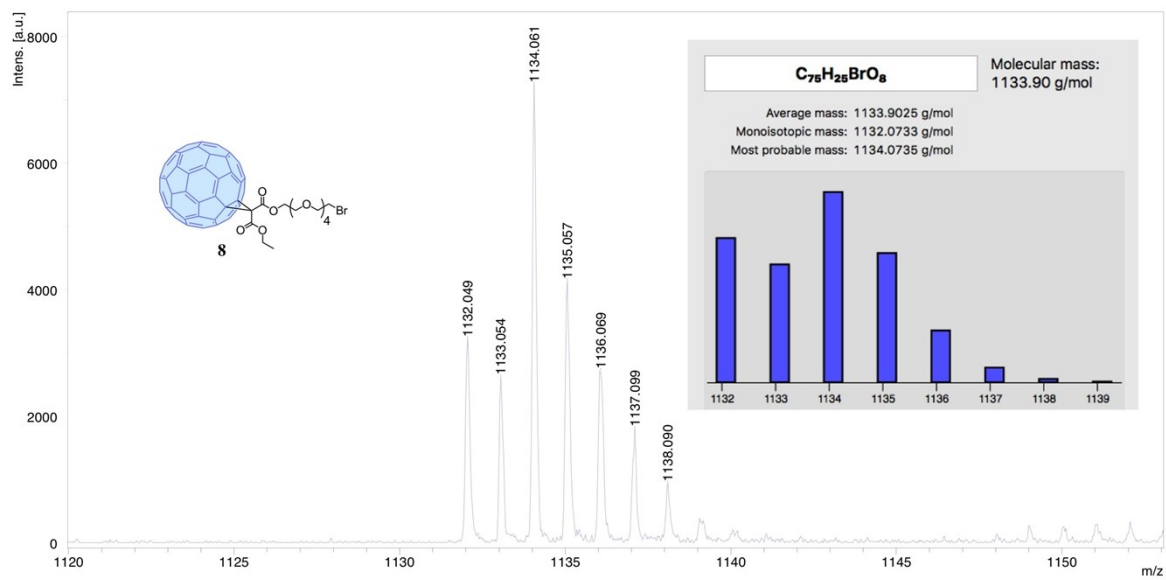


Figure S4e. Experimental and calculated isotopic patterns of compound **8**.

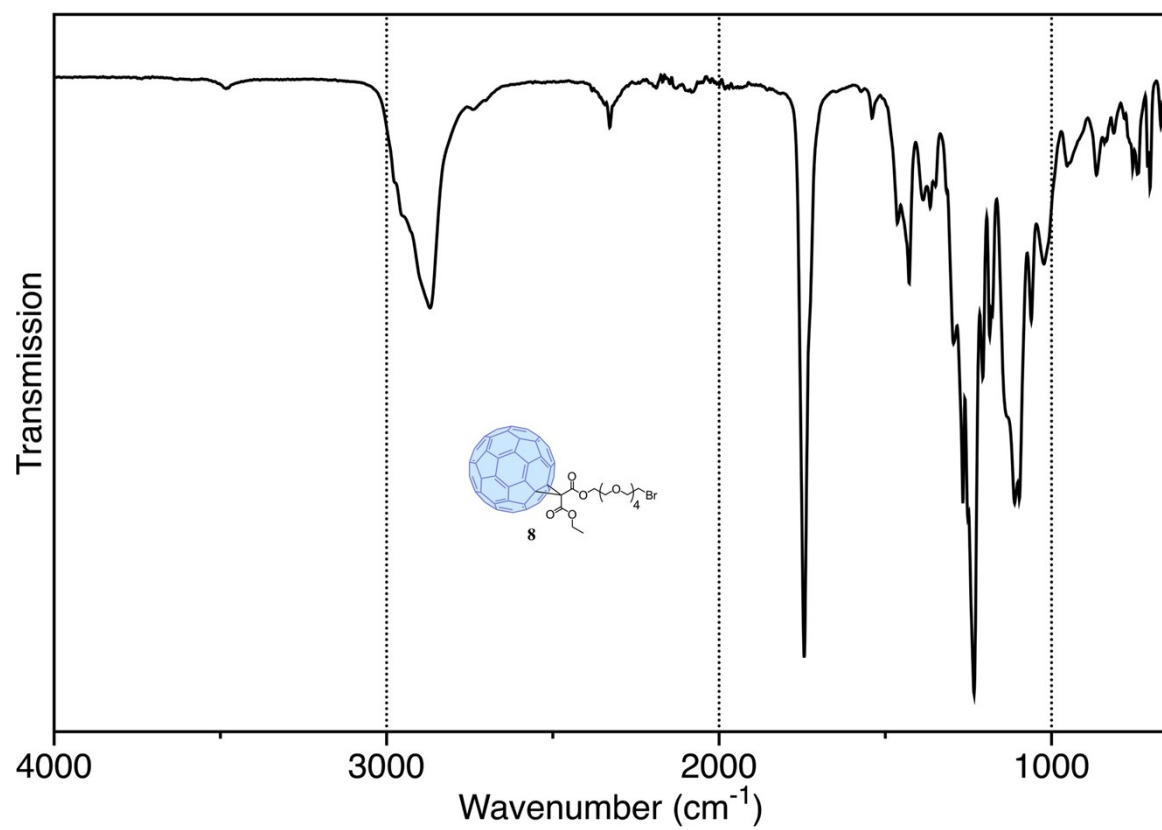


Figure S4f. IR spectrum of compound **8**.

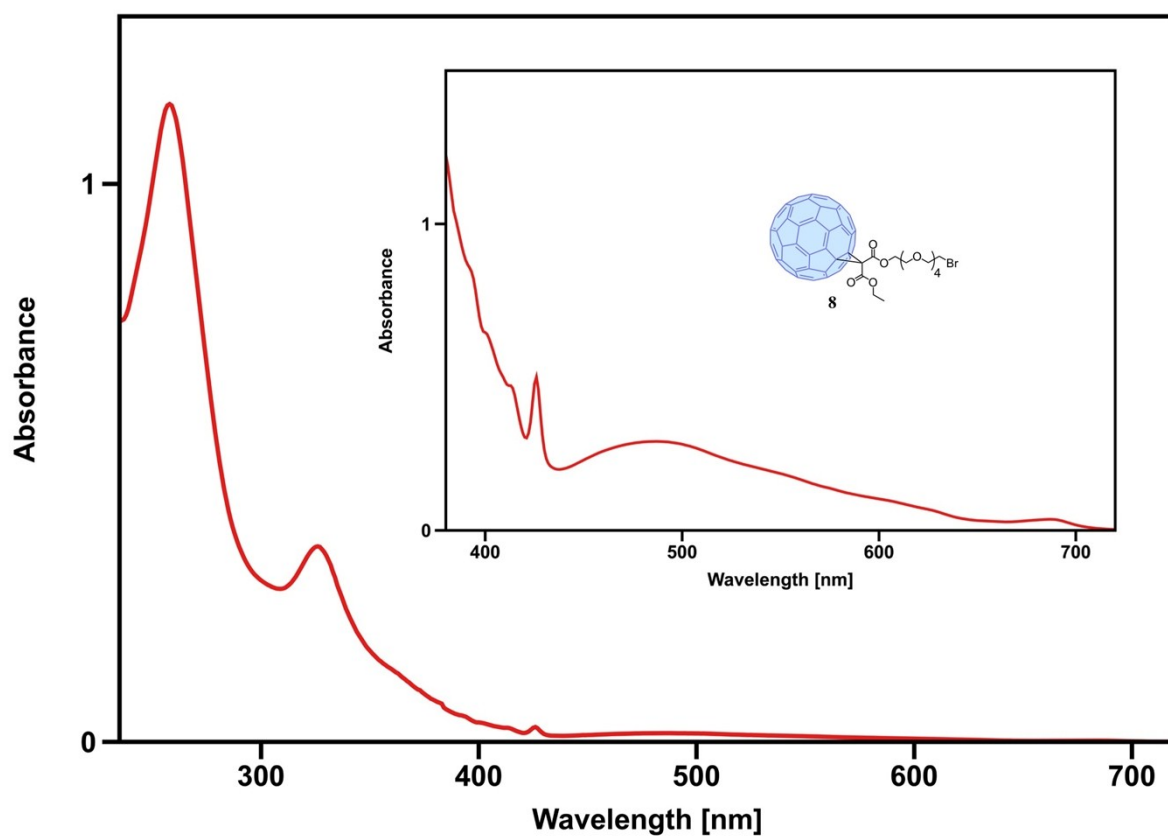


Figure S4g. UV-vis spectrum of compound **8** (CH₂Cl₂).

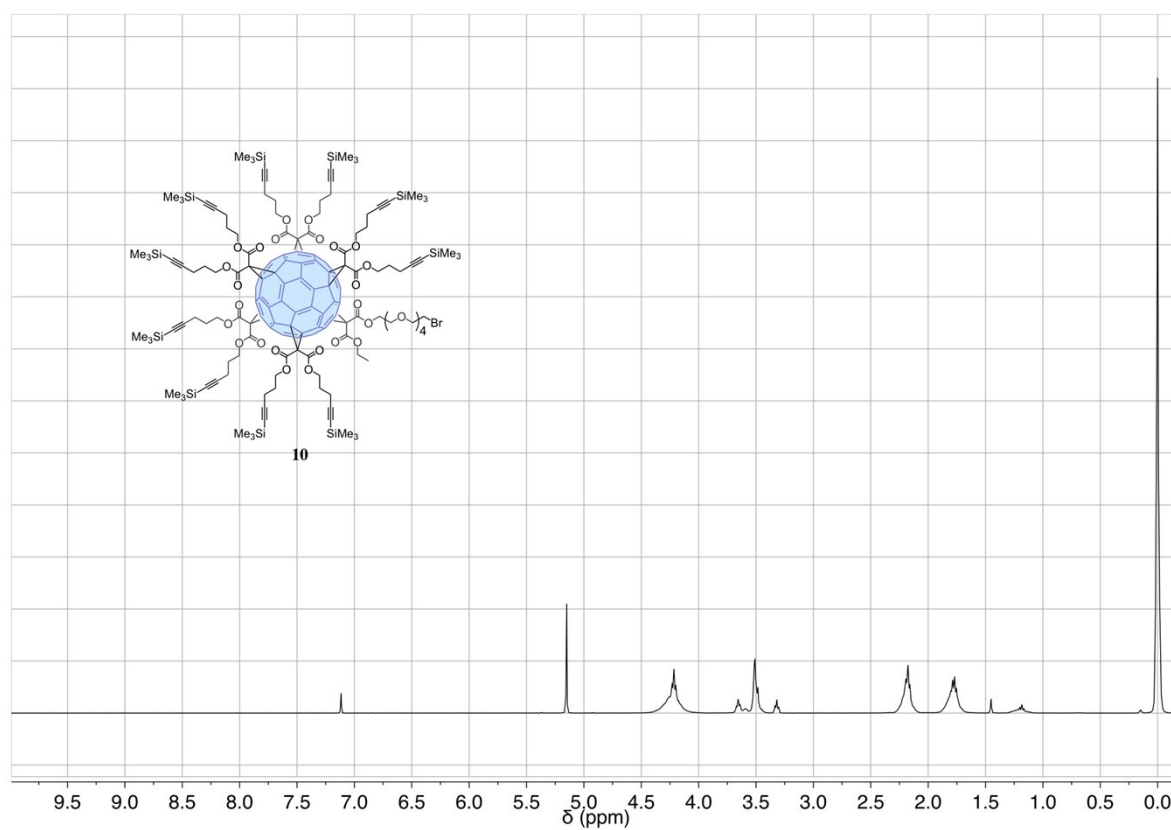


Figure S5a. ¹H NMR spectrum of compound **10** (CDCl₃, 400 MHz).

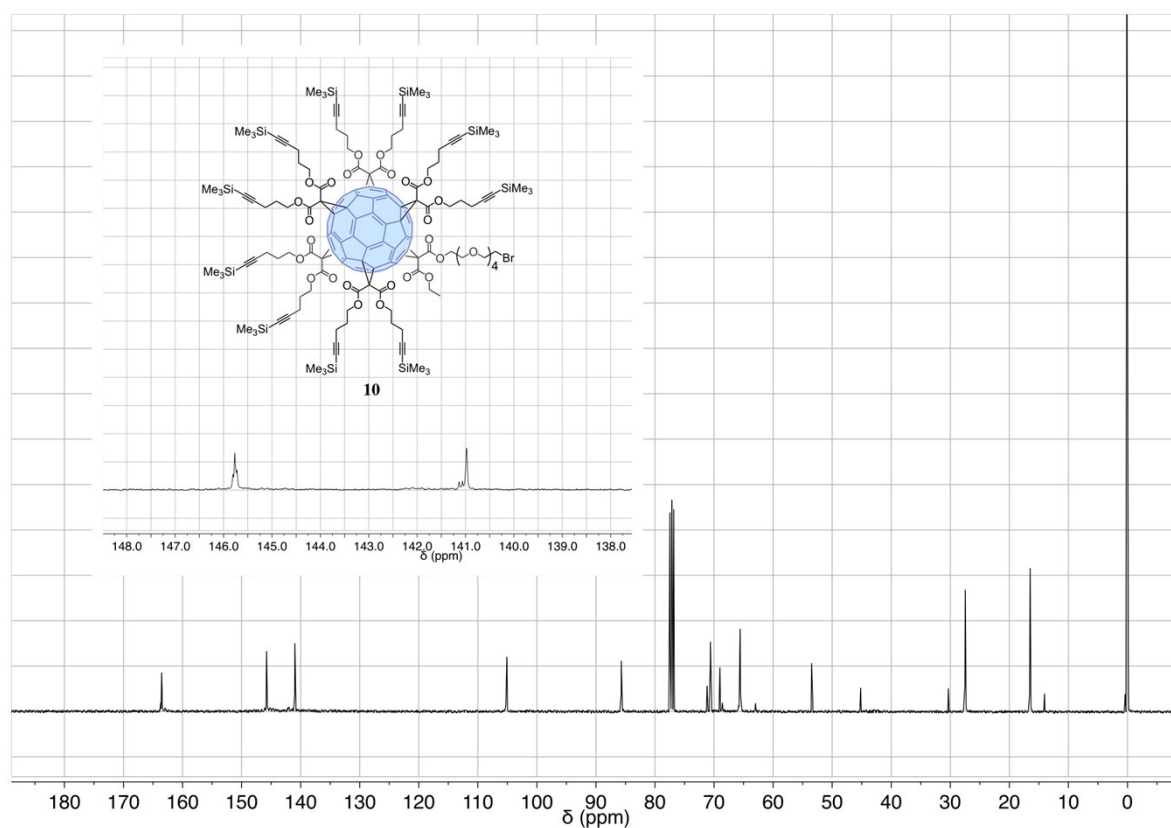


Figure S5b. ¹³C NMR spectrum of compound **10** (CDCl₃, 100 MHz). Close inspection of the fullerene signals revealed a strong influence of the local symmetry. In the ¹³C NMR spectrum of hexa-adduct **10**, three groups of signals appear for the fullerene C atoms at $\delta = 145.7$ (*sp*² C), 141.0 (*sp*² C) and 71.1 (*sp*³ C) ppm reminiscent of those of the three non-equivalent fullerene C atoms of a *T_h*-symmetrical C₆₀ hexa-adduct carrying six identical addends.

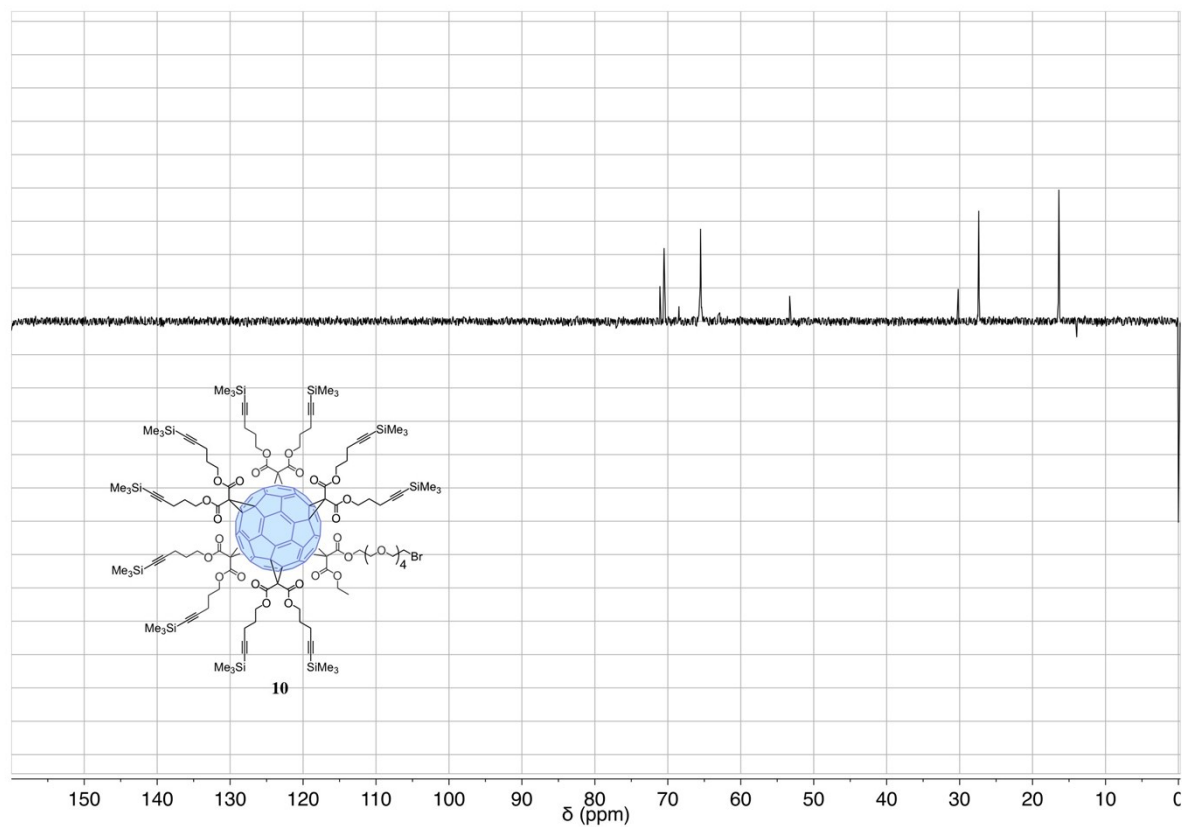


Figure S5c. DEPT spectrum of compound **10** (CDCl₃, 100 MHz).

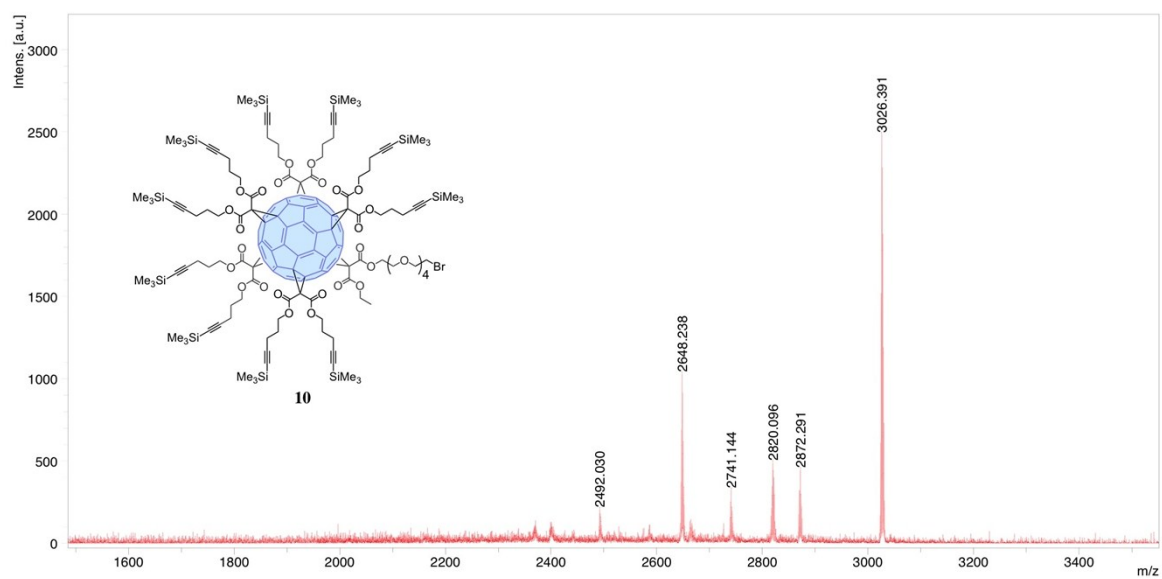


Figure S5d. MALDI-TOF mass spectrum of compound **10**: 3026.4 ($[M]^+$), 2872.3 ($[M-O(CH_2)_3CCTMS]^+$), 2741.1 ($[M-CH_2(CH_2OCH_2)_4CH_2Br]^+$), 2648.2 ($[M-C(CO_2(CH_2)_3CCTMS)_2]^+$), 2492.0 ($[M-C(CO_2(CH_2)_3CCTMS)_2-O(CH_2)_3CCTMS]^+$).

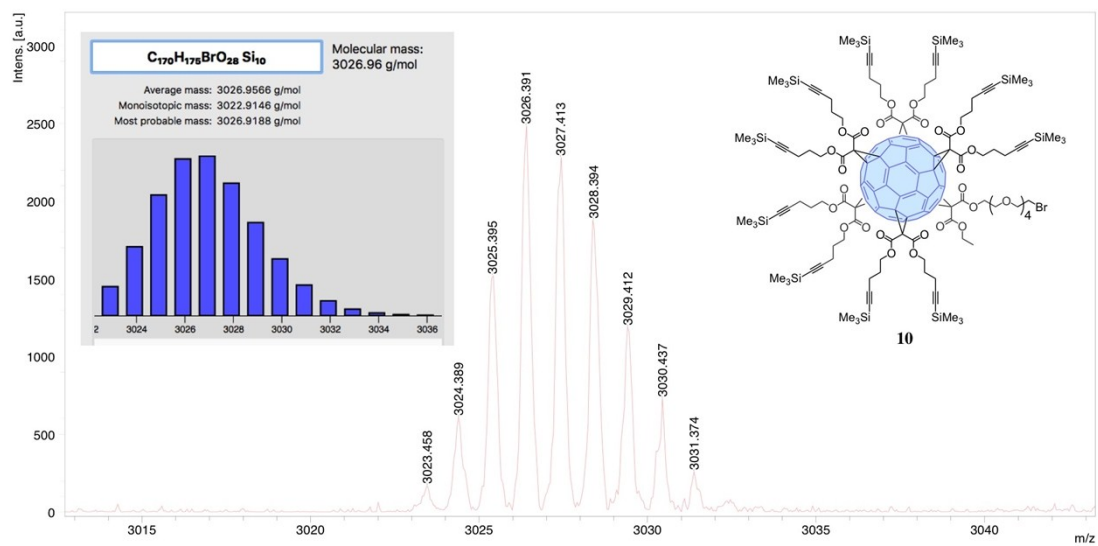


Figure S5e. Experimental and calculated isotopic patterns of compound **10**.

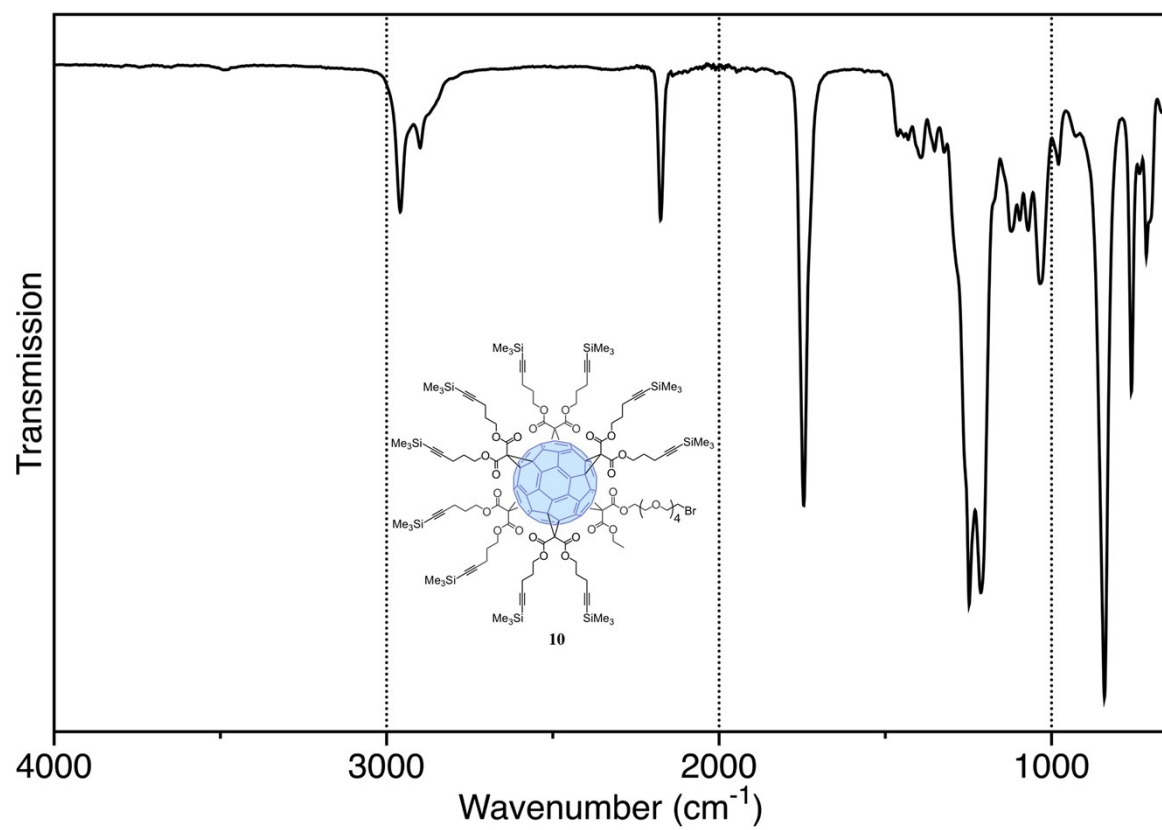


Figure S5f. IR spectrum of compound **10**.

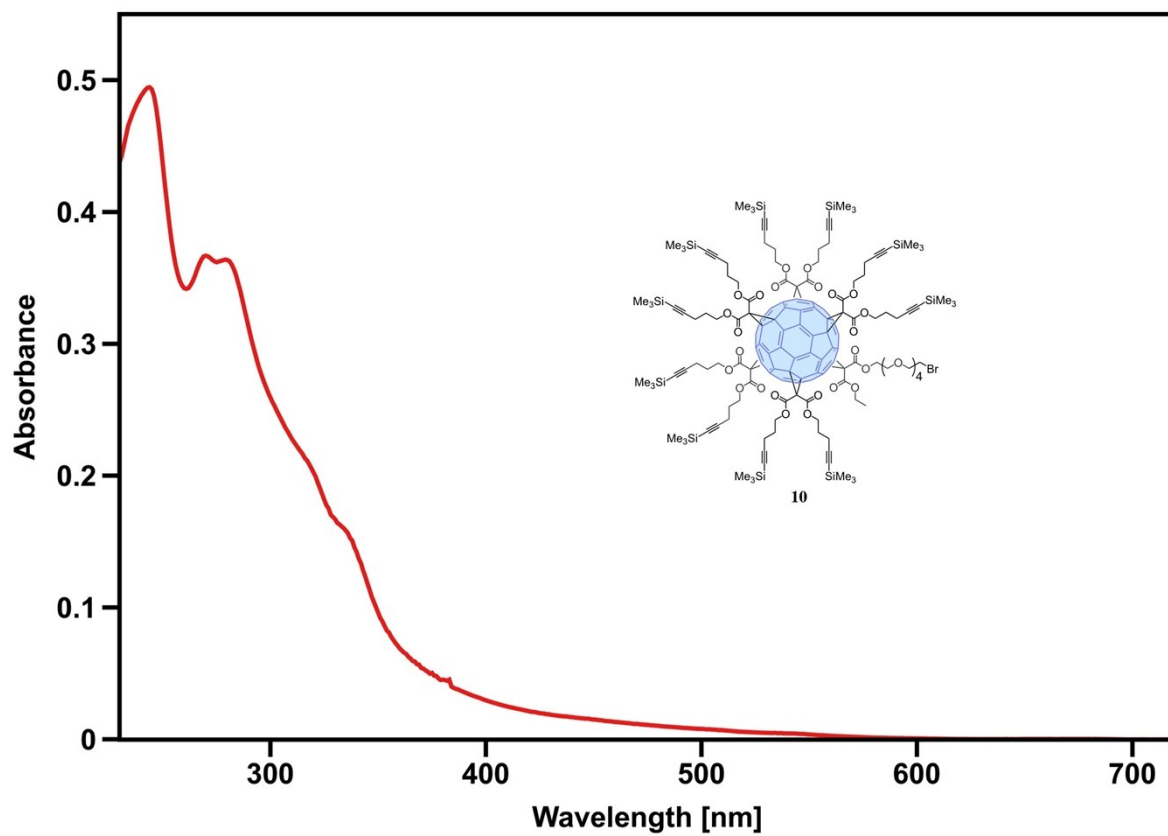


Figure S5g. UV-vis spectrum of compound **10** (CH₂Cl₂).

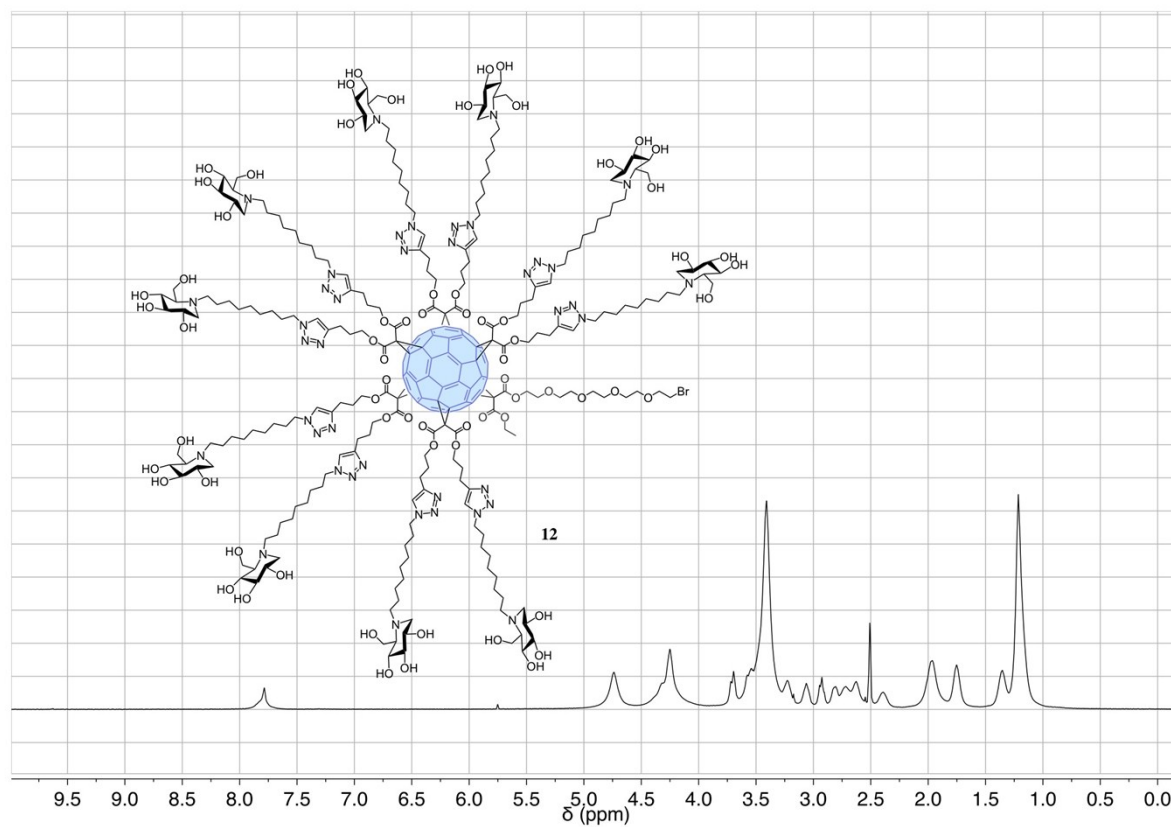


Figure S6a. ^1H NMR spectrum of compound **12** (DMSO-*d*₆, 400 MHz).

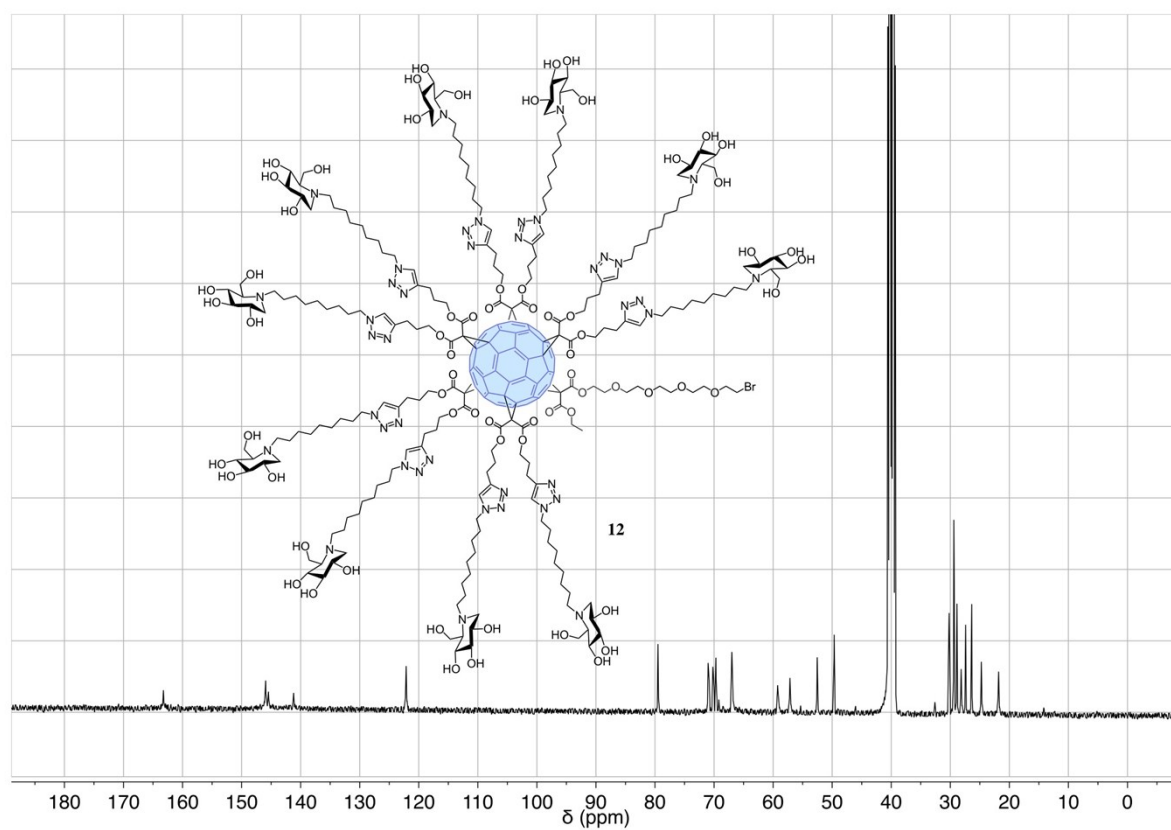


Figure S6b. ^{13}C NMR spectrum of compound **12** (DMSO-*d*₆, 100 MHz).

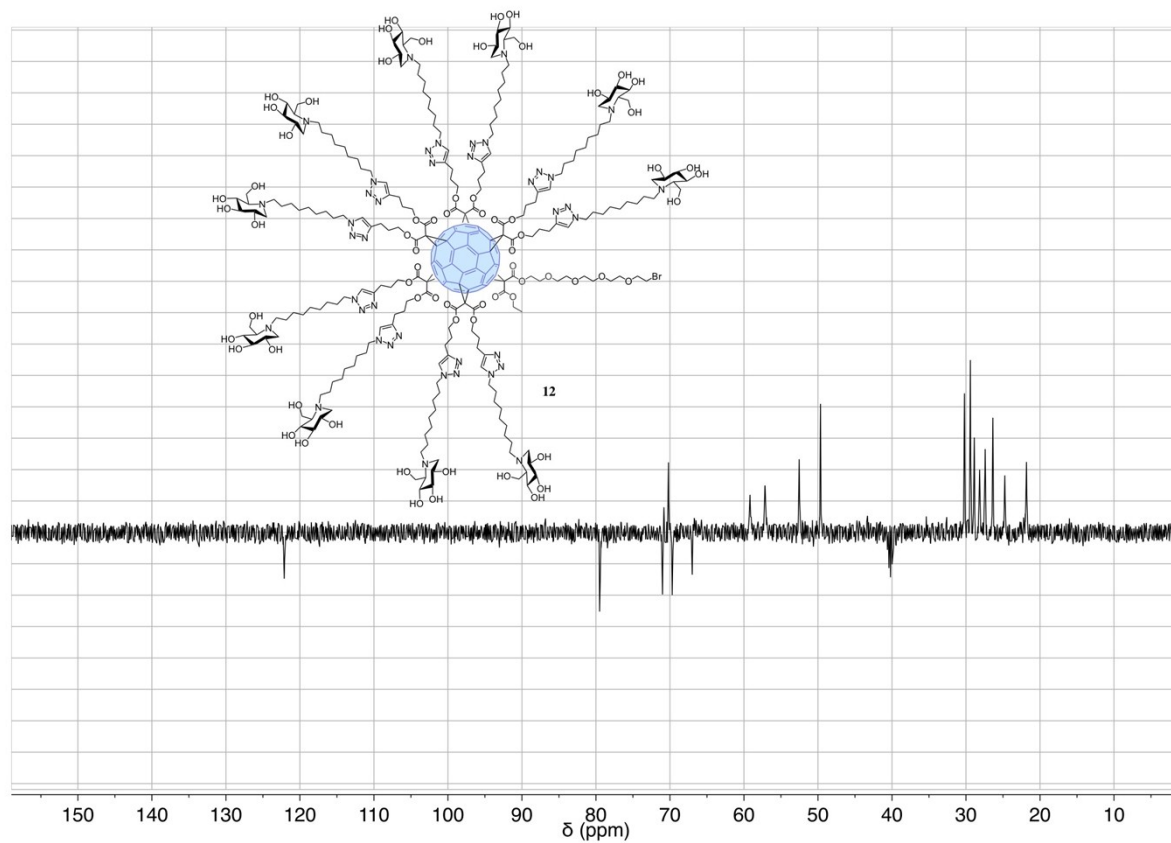


Figure S6c. DEPT spectrum of compound **12** (DMSO-*d*₆, 100 MHz).

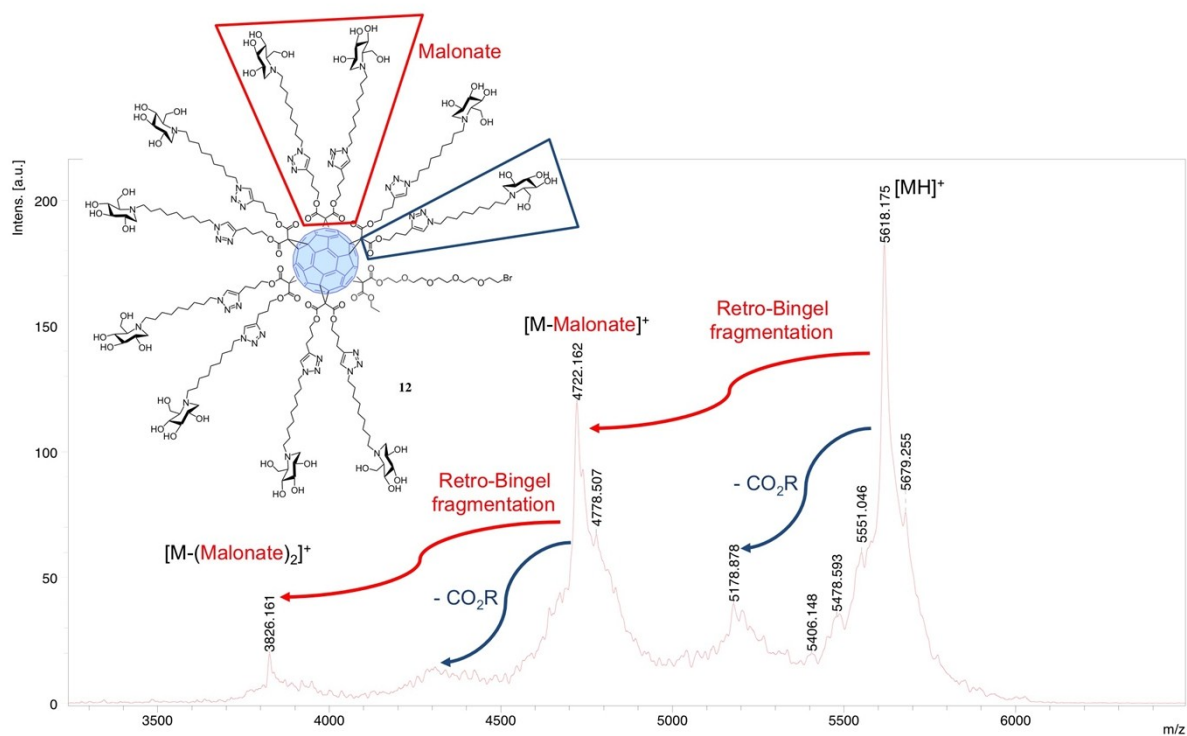


Figure S6d. MALDI-TOF mass spectrum of compound 12.

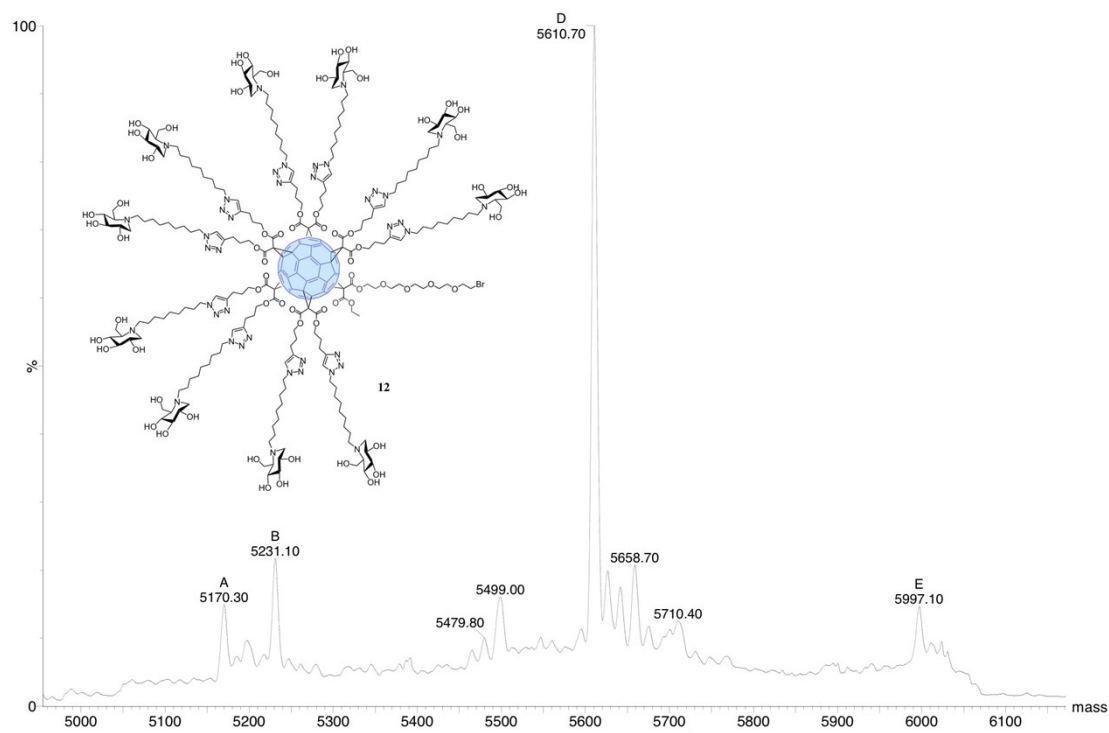


Figure S6e. ESI-TOF mass spectrum of compound **12**.

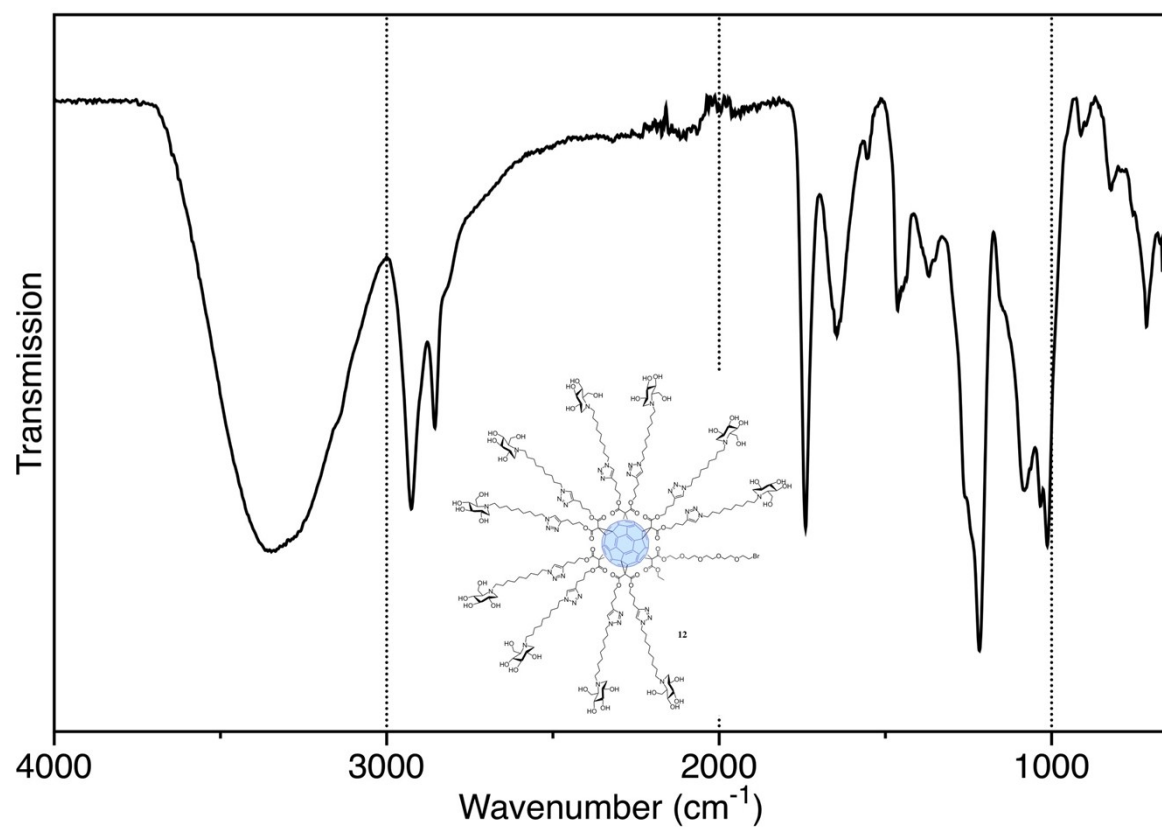


Figure S6f. IR spectrum of compound 12.

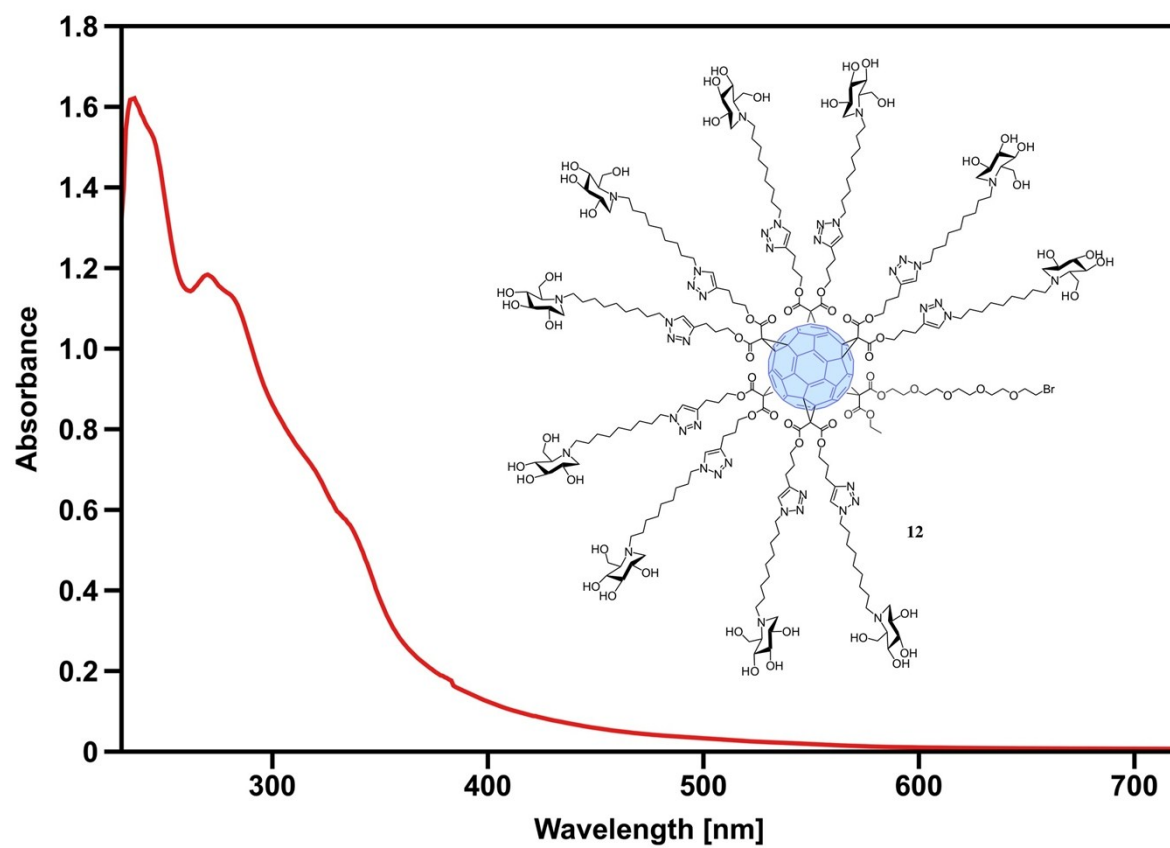


Figure S6g. UV-vis spectrum of compound **12** (H₂O/DMSO 10/0.2).

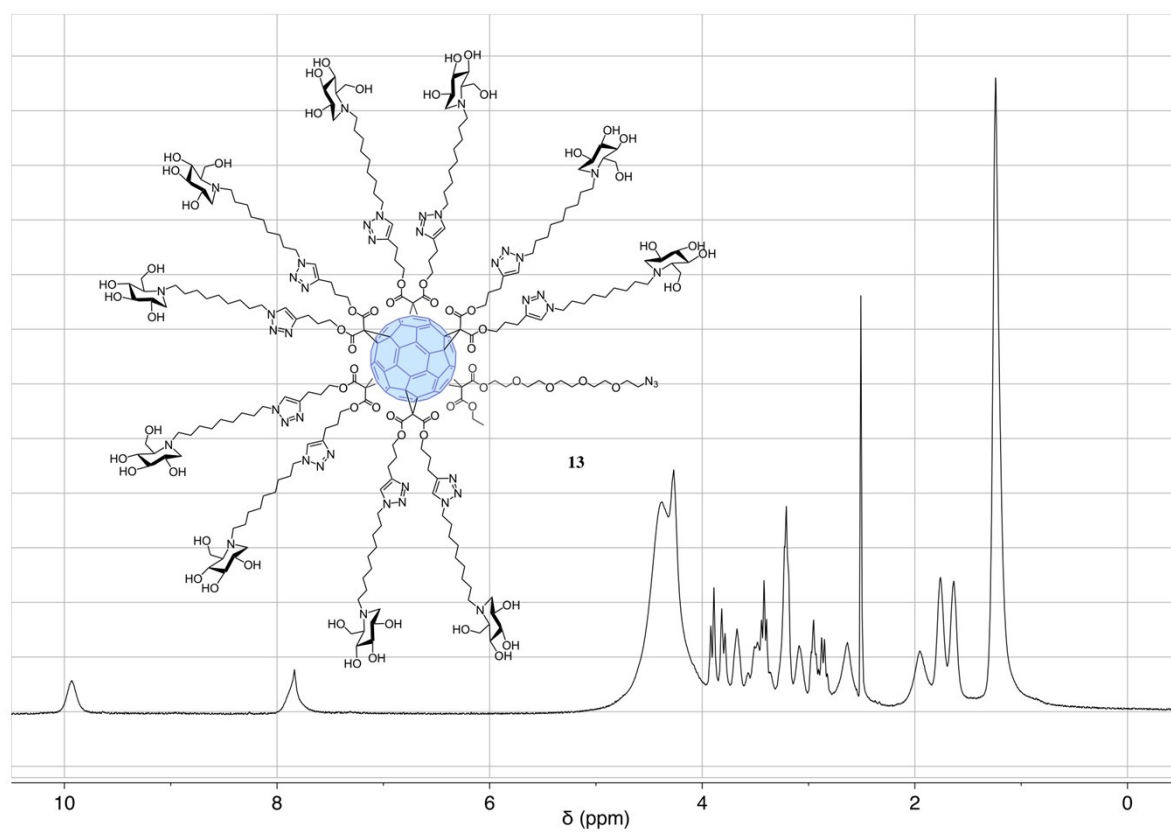


Figure S7a. ^1H NMR spectrum of compound **13** ($\text{DMSO-}d_6$, 400 MHz). The sample was treated with aqueous HCl to improve the solubility.

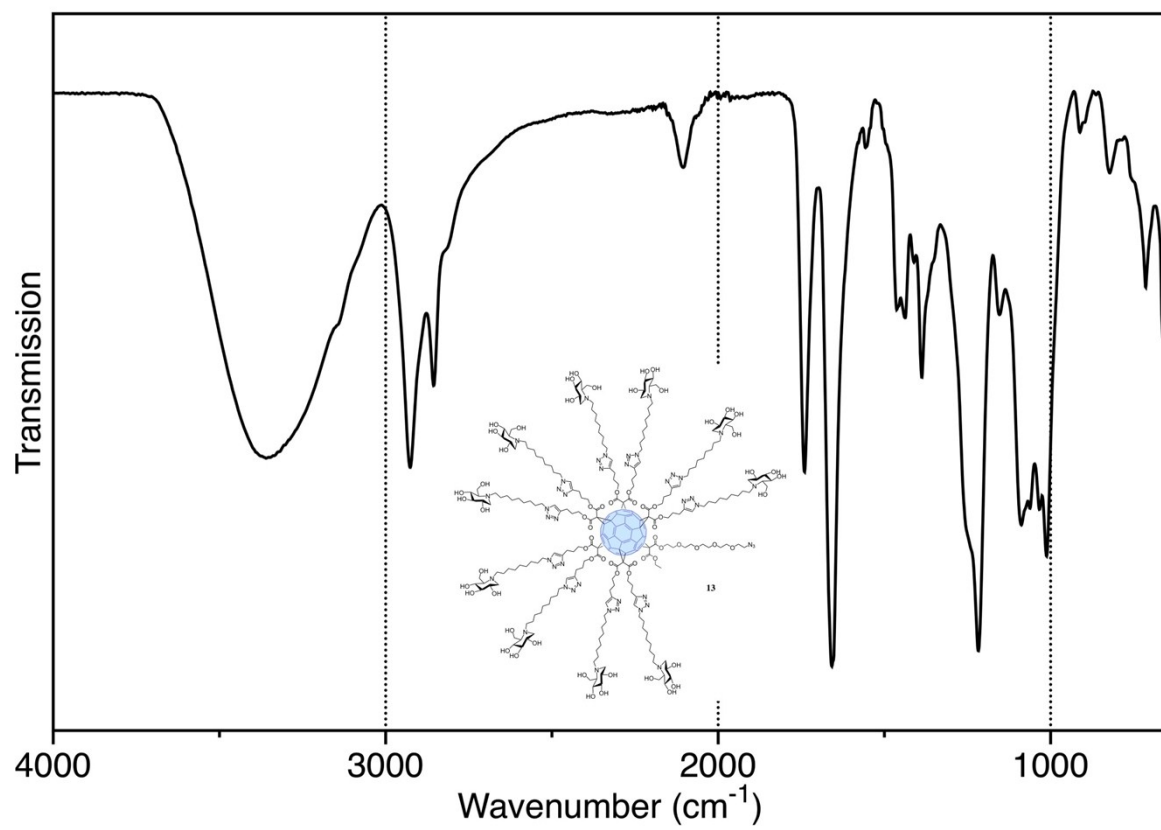


Figure S7b. IR spectrum of compound **13**.

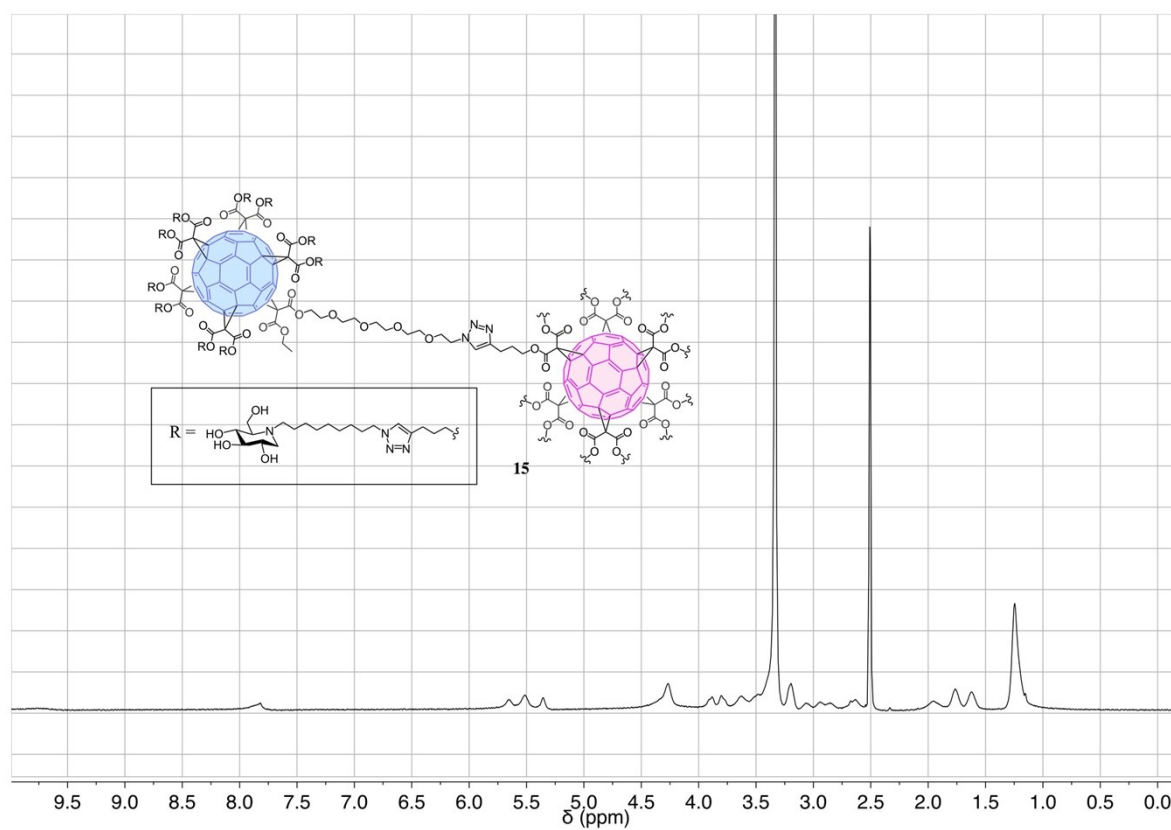


Figure S8a. ¹H NMR spectrum of compound **15** (DMSO-*d*₆, 400 MHz). The sample was treated with aqueous HCl to improve the solubility.

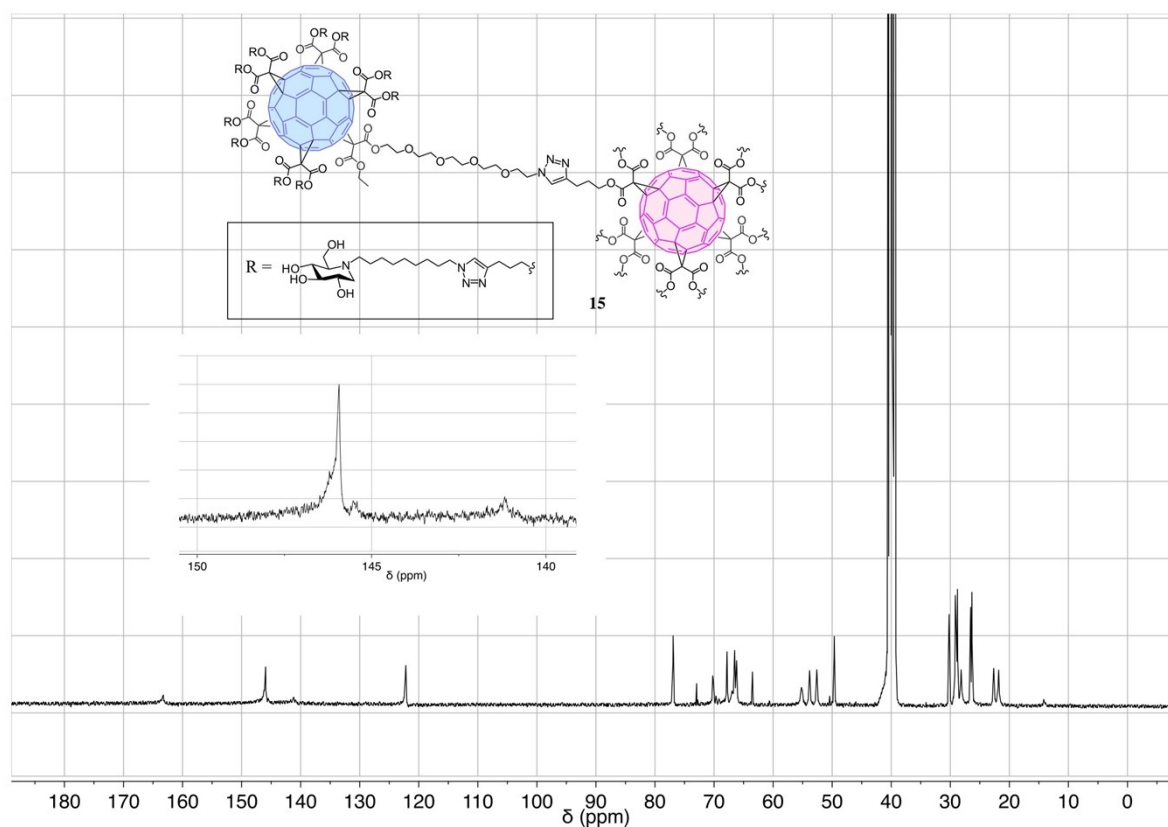


Figure S8b. ^{13}C NMR spectrum of compound **15** (DMSO-*d*₆, 100 MHz).

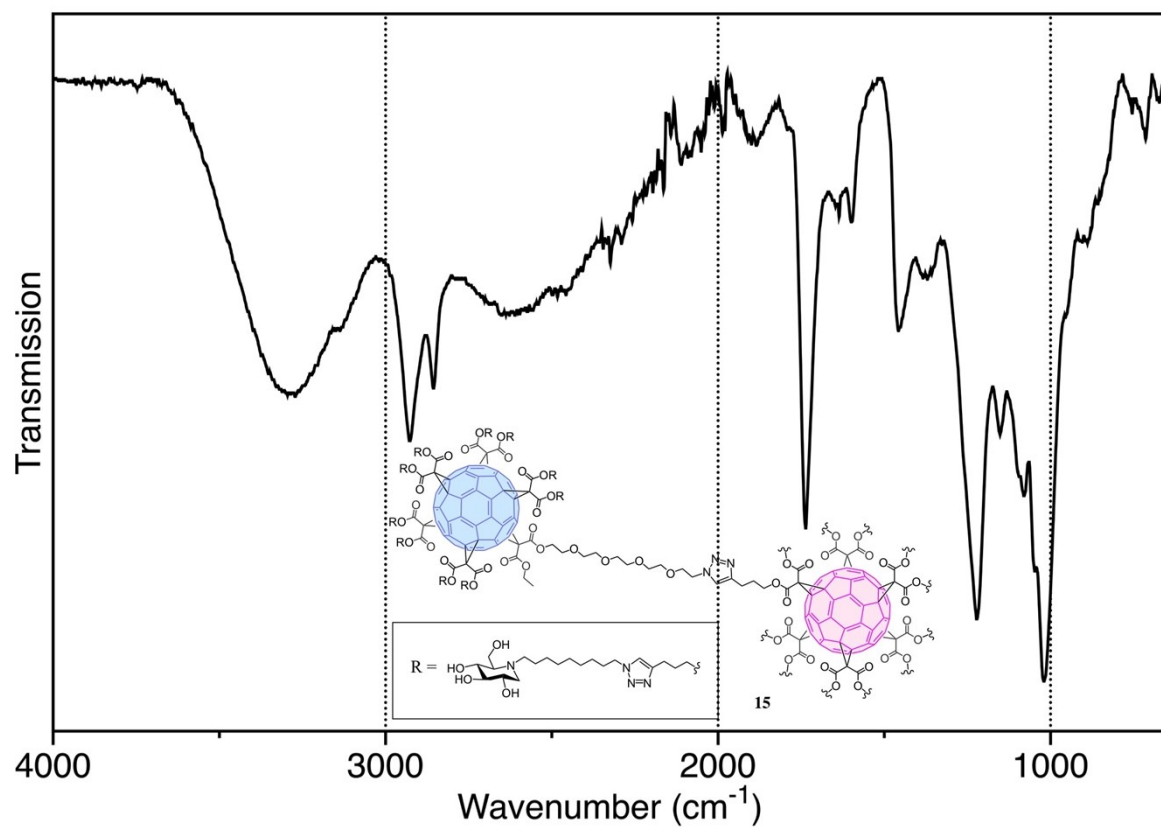


Figure S8c. IR spectrum of compound 15.

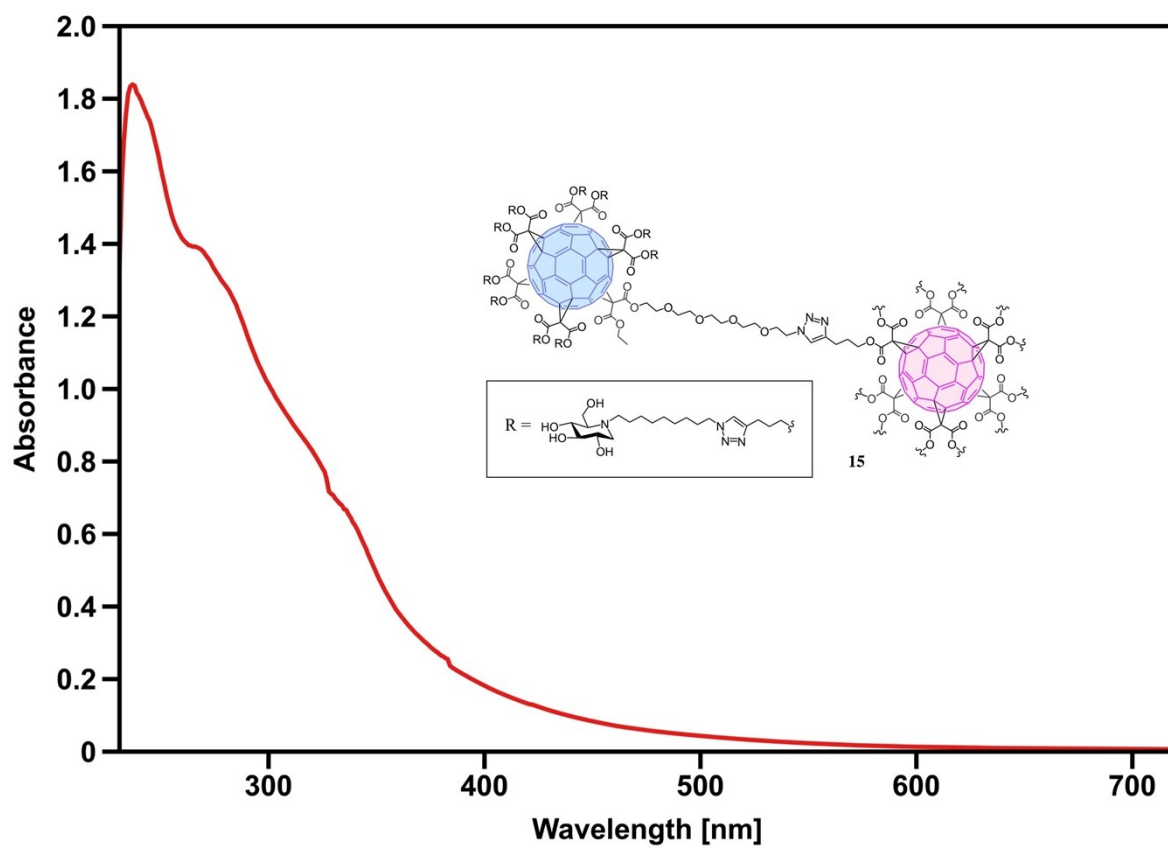


Figure S8d. UV-vis spectrum of compound 15 (H₂O/DMSO 10/0.2).

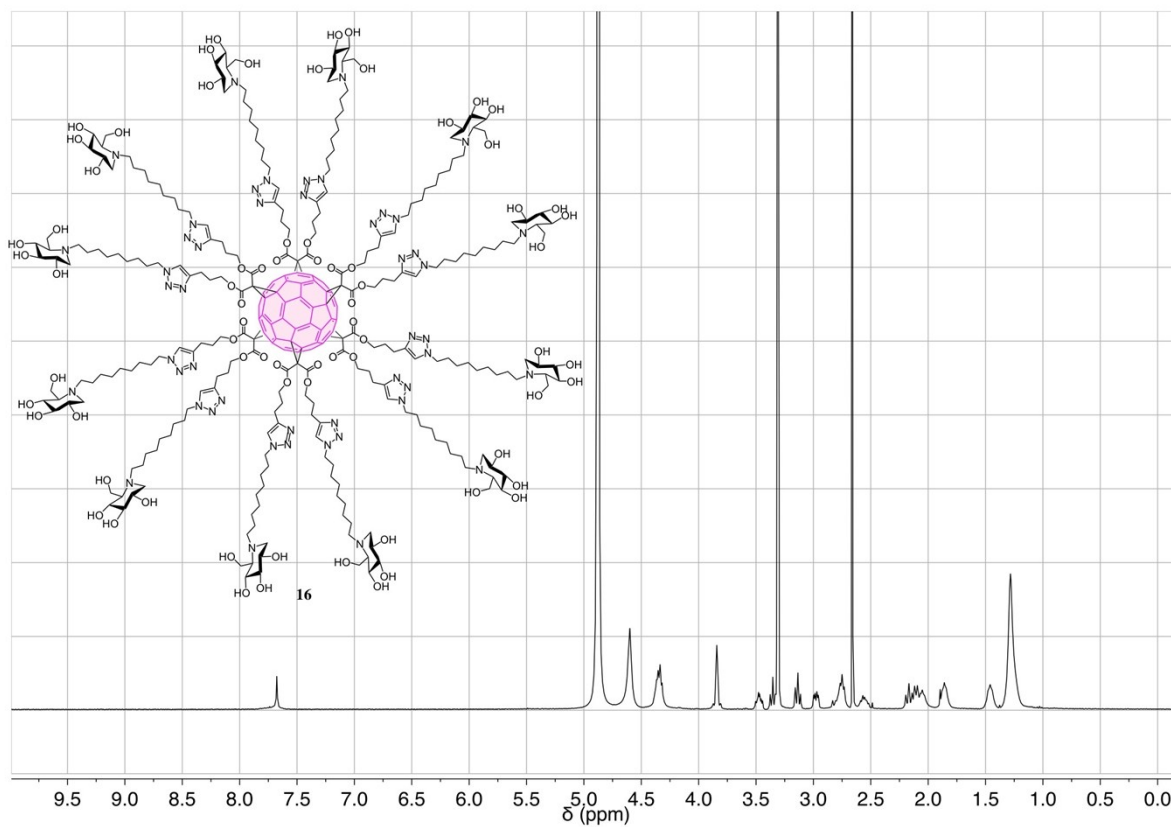


Figure S9a. ^1H NMR spectrum of compound **16** (CD_3OD , 400 MHz).

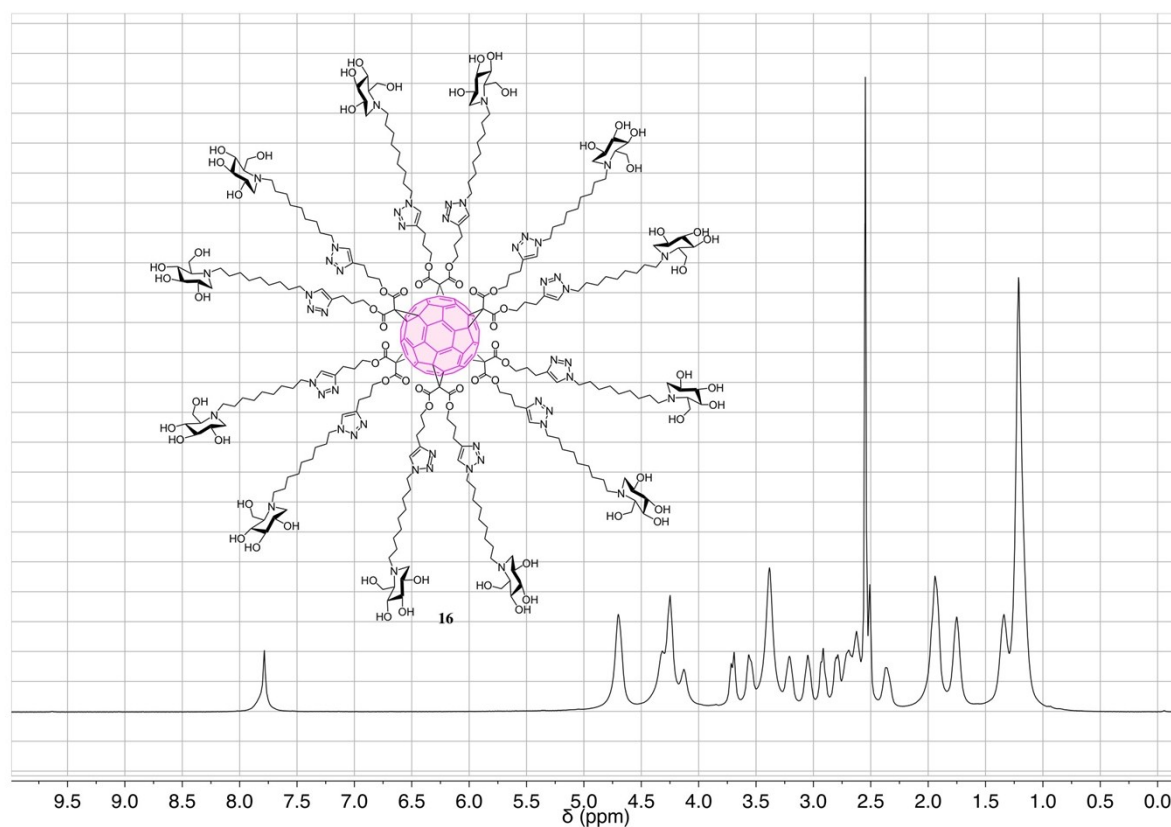


Figure S9b. ^1H NMR spectrum of compound **16** ($\text{DMSO-}d_6$, 400 MHz).

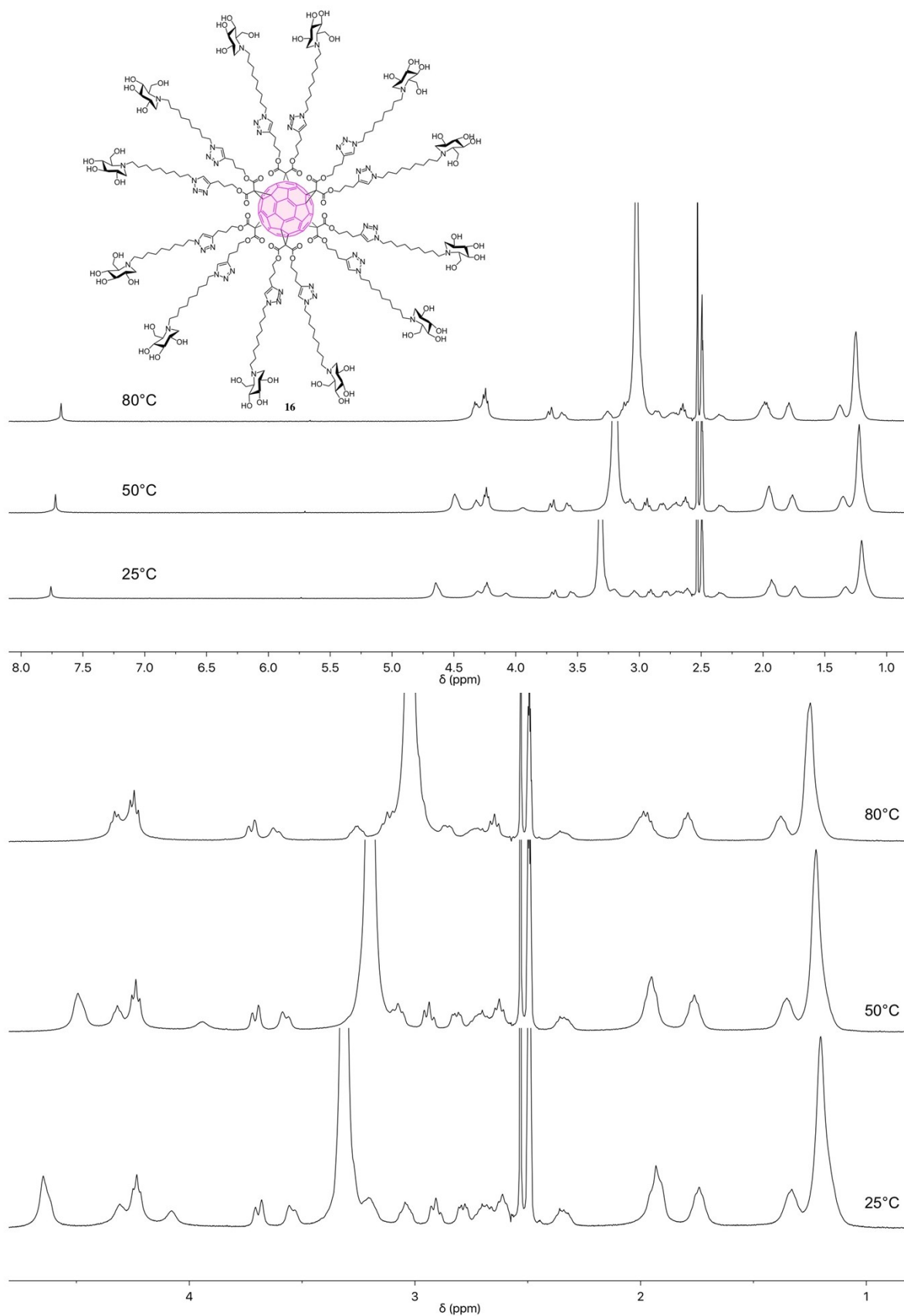


Figure S9c. ¹H NMR spectra of compound **16** (DMSO-*d*₆, 400 MHz) recorded at different temperatures.

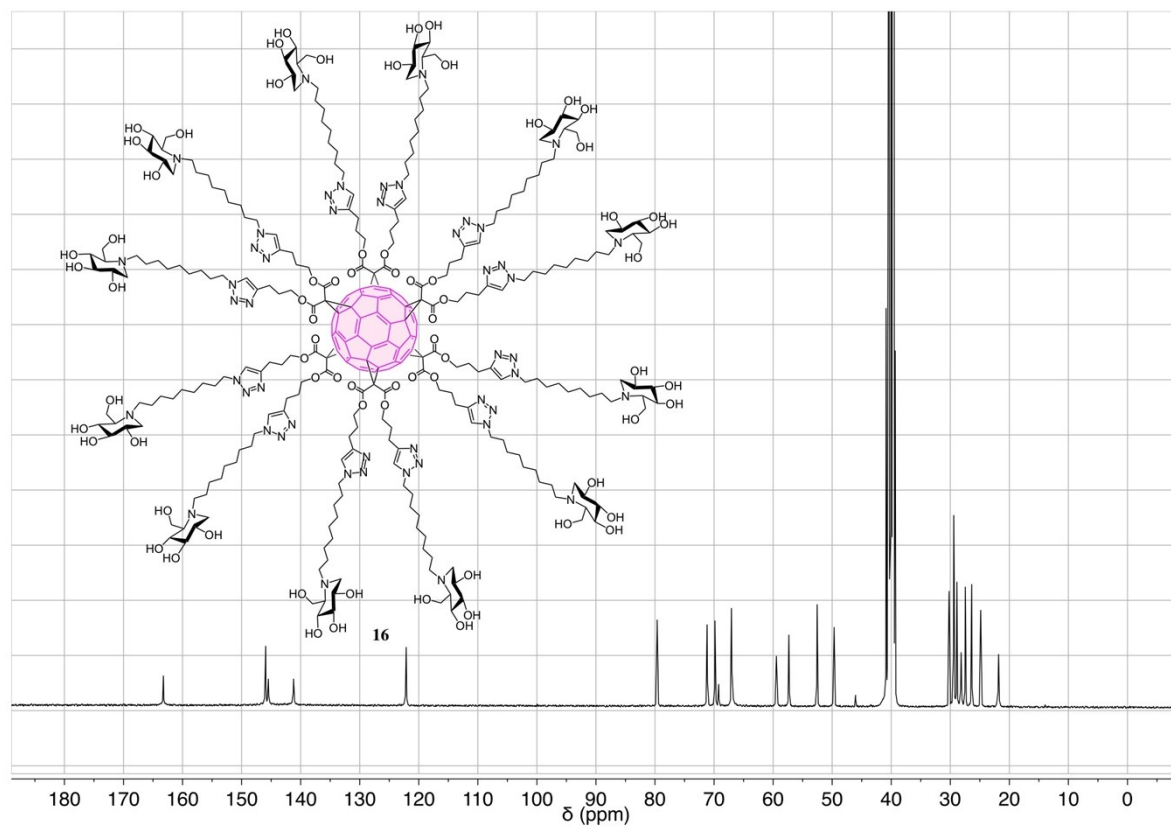


Figure S9d. ¹³C NMR spectrum of compound 16 (DMSO-*d*₆, 100 MHz).

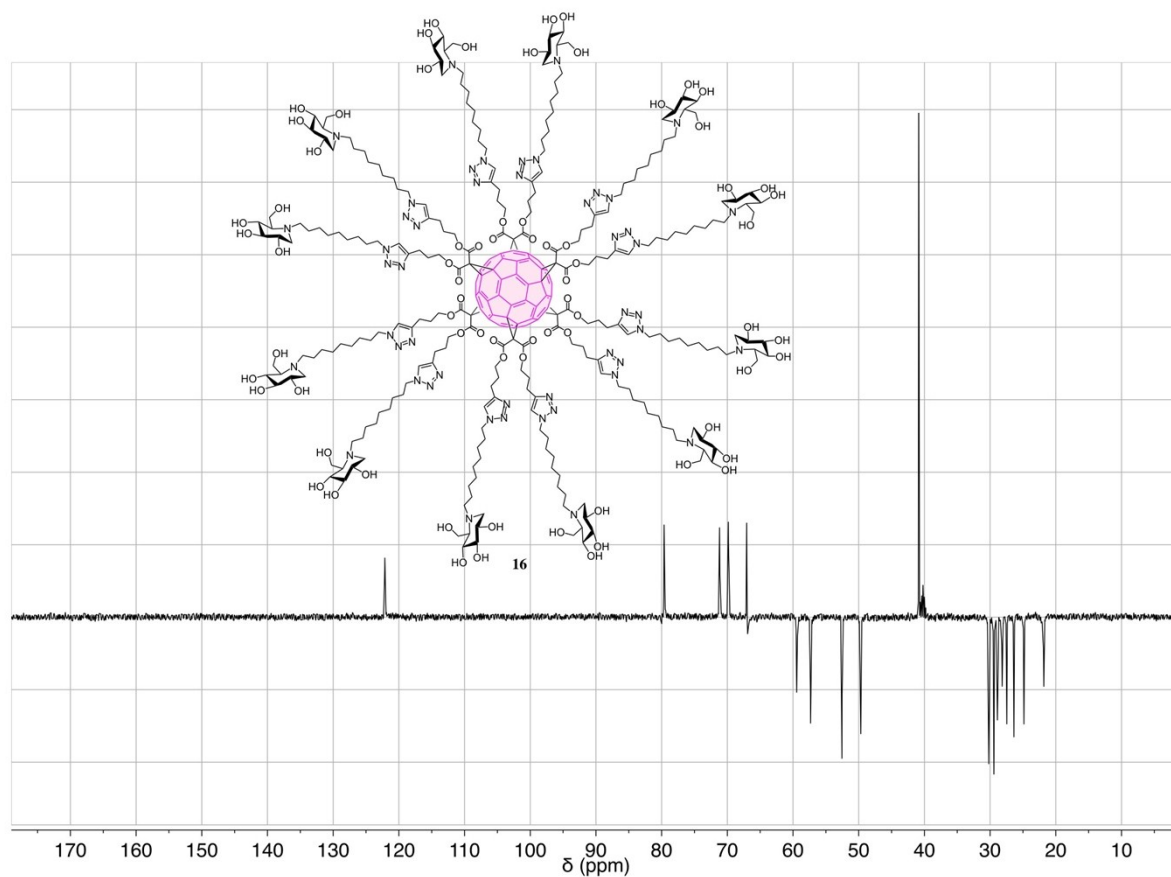


Figure S9e. DEPT spectrum of compound **16** (CDCl₃, 100 MHz).

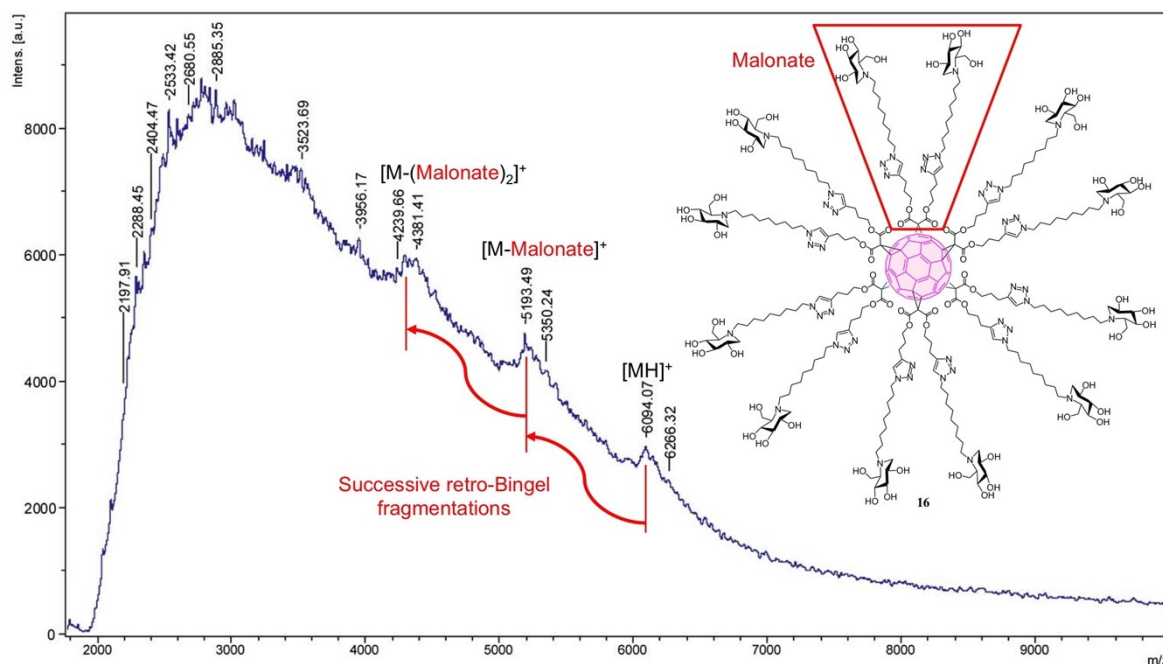


Figure S9f. MALDI-TOF mass spectrum of compound **16**. The analysis of this compound was found particularly difficult due to the formation of matrix adducts explaining the broad and featureless noise signal. However, the expected molecular ion peak as well as characteristic fragments can be observed. Similar effects have been already observed for related glycofullerenes.¹

¹ S. Cecioni, V. Oerthel, J. Iehl, M. Holler, D. Goyard, J.-P. Praly, A. Imbert, J.-F. Nierengarten, S. Vidal, *Chem. Eur. J.* **2011**, *17*, 3252-3261.

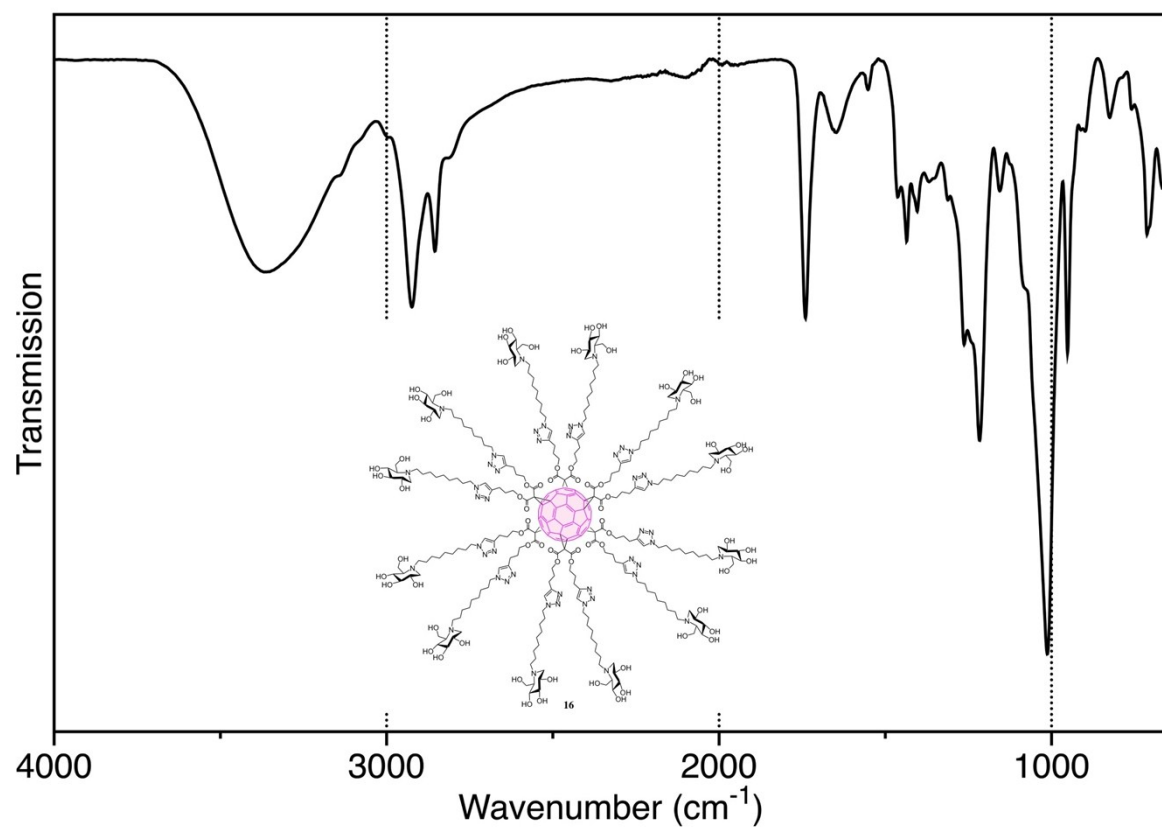


Figure S9g. IR spectrum of compound **16**.

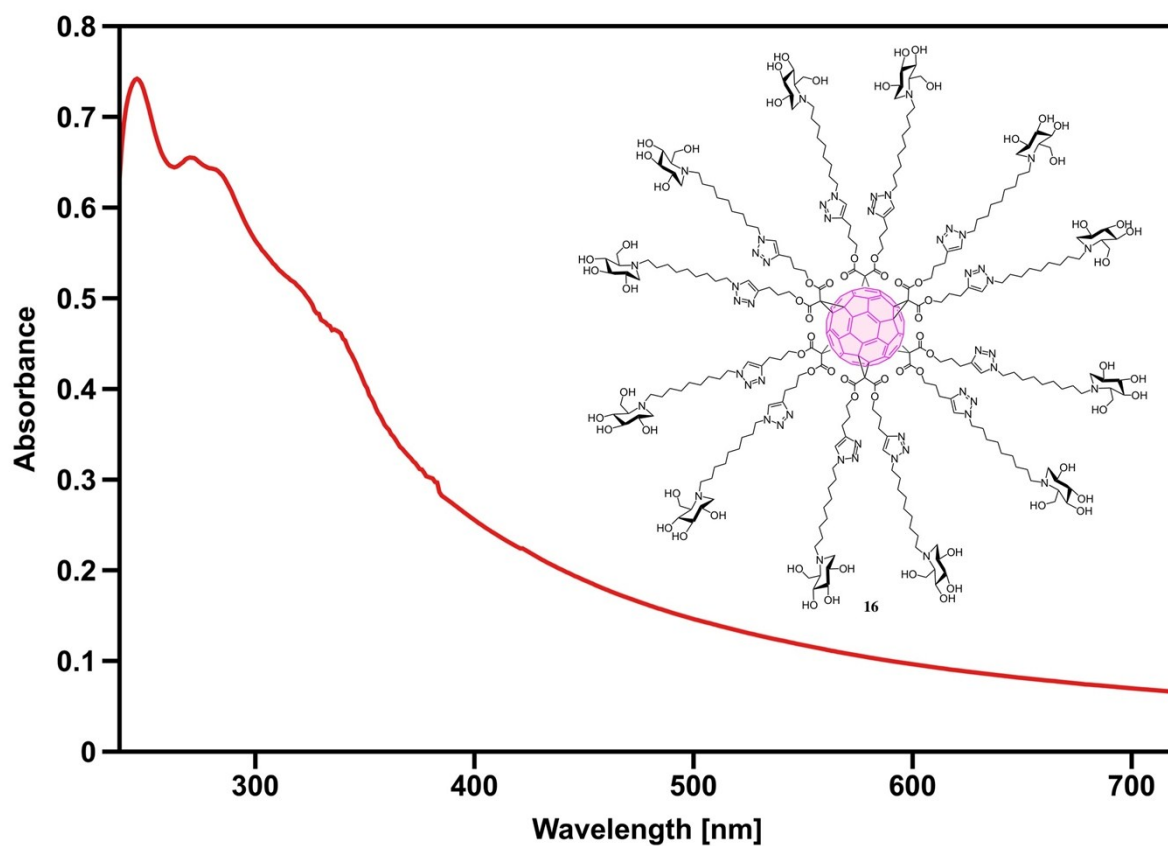


Figure S9h. UV-vis spectrum of compound 16 (H₂O/DMSO 10/0.2).

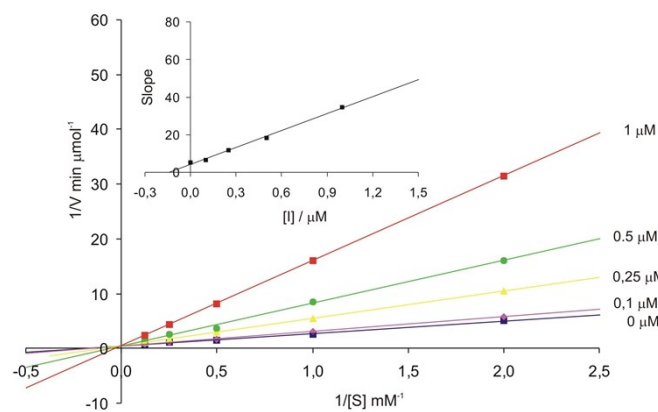


Figure S10a. Lineweaver-Burk Plot for K_i determination (0.14 μM) of 15 against amyloglucosidase (*Aspergillus niger*).

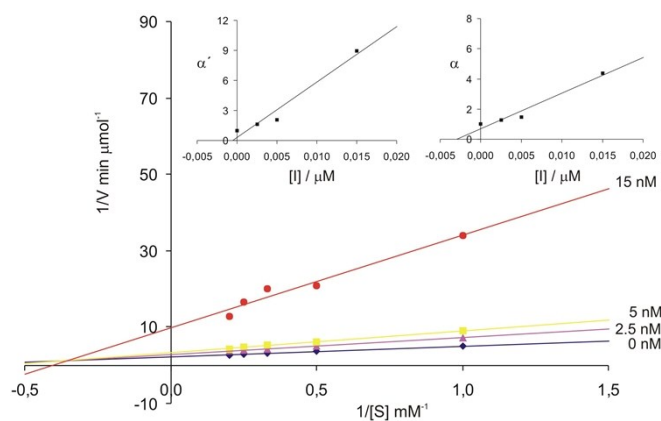


Figure S10b. Lineweaver-Burk Plot for K_i and K'_i determination (0.0018 and 0.0042 μM) of **15** against α -mannosidase (jack bean).

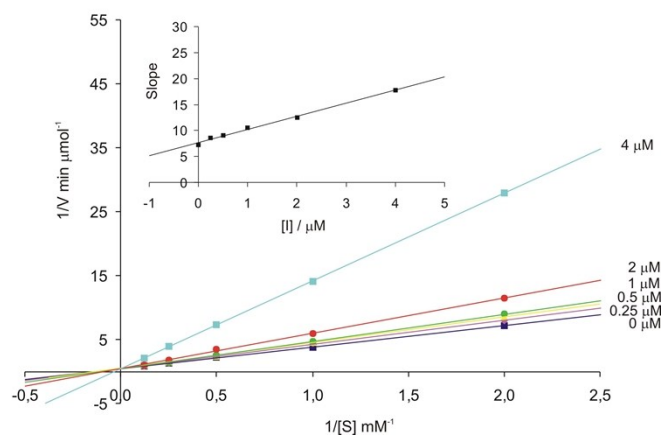


Figure S11a. Lineweaver-Burk Plot for K_i determination (3.0 μM) of **16** against amyloglucosidase (*Aspergillus niger*).

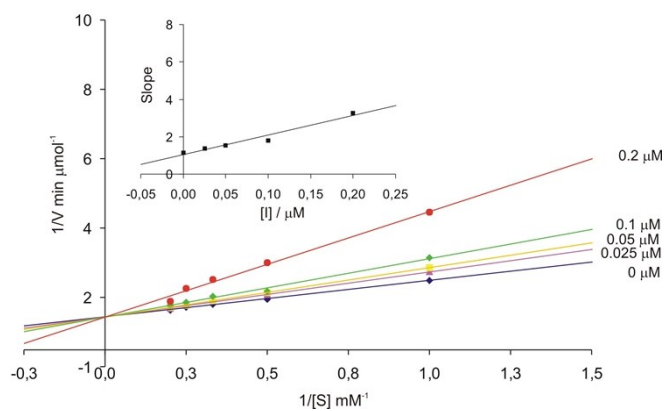


Figure S11b. Lineweaver-Burk Plot for K_i determination (0.099 μM) of **16** against α -mannosidase (jack bean).

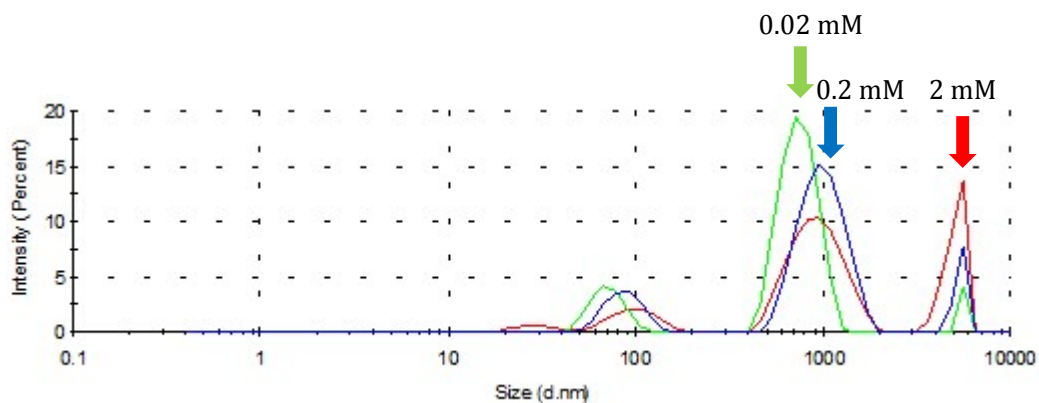


Figure S12. DLS analysis of fullerene 16. DLS measurements in H₂O-DMSO 3:7 at 0.02, 0.2 and 2 mM

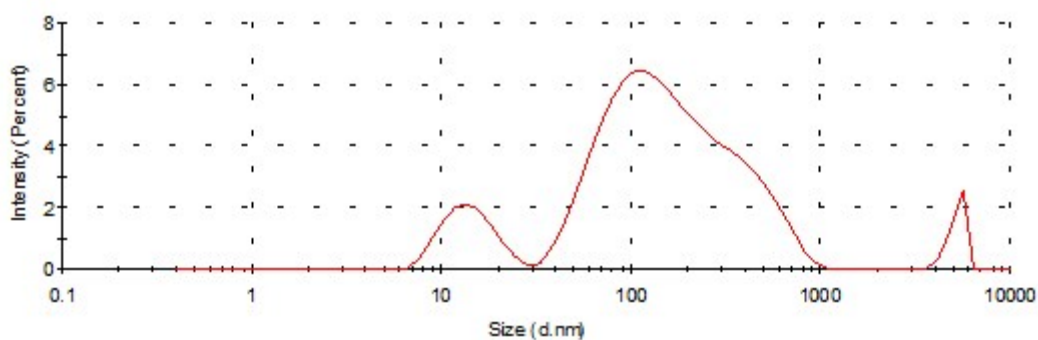


Figure S13a. DLS analysis of tridecafullerene 15. DLS measurement in MilliQ water (1.15 mg mL⁻¹).

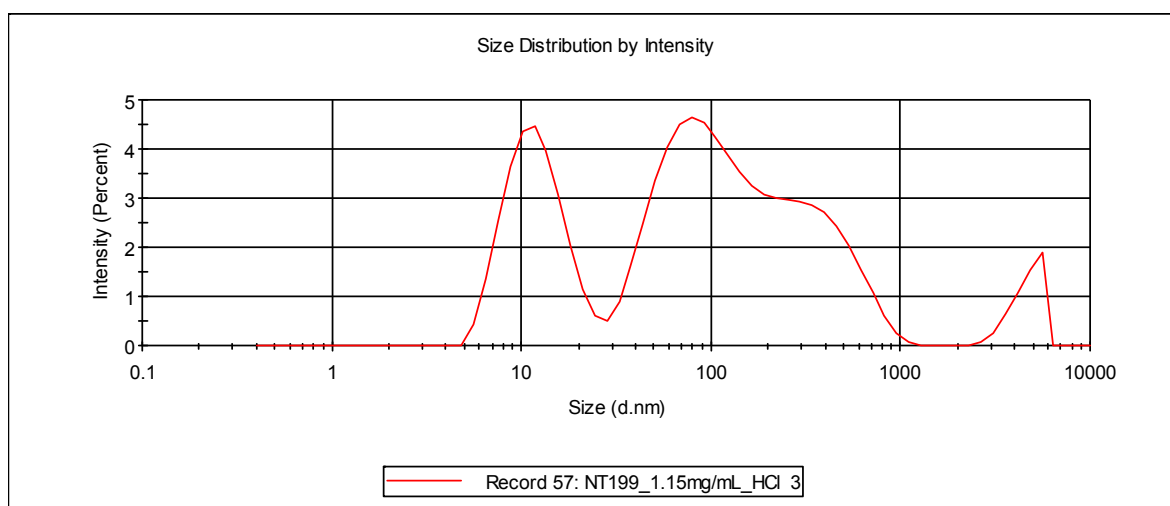


Figure S13b. DLS analysis of tridecafullerene 15. DLS measurement in MilliQ water (1.15 mg mL⁻¹) after acidification with HCl 0.1 M (pH 1-2),